Closed-loop Control of Functional Neuromuscular Stimulation

NIH Neuroprosthesis Program Contract Number N01-NS-6-2338
Quarterly Progress Report #2
May 1, 1996 to September 30, 1996

Investigators:
Patrick E. Crago, Ph.D.
Clayton Van Doren, Ph.D.
Warren M. Grill, Ph.D.
Michael W. Keith, M.D.
Kevin Kilgore, Ph.D.
Joseph Mansour, Ph.D.
P. Hunter Peckham, Ph.D.
David Wilson, Ph.D.

Departments of
Biomedical Engineering,
Mechanical and Aerospace Engineering,
and Orthopaedics
Case Western Reserve University
and MetroHealth Medical Center

This QPR is being sent to you before it has been reviewed by the staff of the Neural Prosthesis Program.

Table of Contents

1. SYNTHESIS OF UPPER EXTREMITY FUNCTION

The overall goals of this project are (1) to measure the biomechanical properties of the neuroprosthesis user's upper extremity and incorporate those measurements into a complete model with robust predictive capability, and (2) to use the predictions of the model to improve the grasp output of the hand neuroprosthesis for individual users.

1. a. BIOMECHANICAL MODELING: PARAMETERIZATION AND VALIDATION

Purpose

In this section of the contract, we will develop methods for obtaining biomechanical data from individual persons. Individualized data will form the basis for model-assisted implementation of upper extremity FNS. Using individualized biomechanical models, specific treatment procedures will be evaluated for individuals The person-specific parameters of interest are tendon moment arms and lines of action, passive moments, and maximum active joint moments. Passive moments will be decomposed into components arising from stiffness inherent to a joint and from passive stretching of muscle-tendon units that cross one or more joints.

Report of progress

1. a. i. MOMENT ARMS VIA MAGNETIC RESONANCE IMAGING

Abstract

A computer program is created to measure tendon moment arm from high resolution 3D MRI images. The method is a 3D geometric method that complements our previous method consisting of the tendon excursion method previously developed. Image data are acquired on an MRI system with unique capabilities for biomechanical imaging. On a volunteer, we measured a tendon moment arm of 13.2 mm for the flexor profundus tendon of the 3rd MCP joint. Measurements showed remarkable consistency with 3 independent measurements of moment arm being 12.45, 14.9, and 13.25 mm for joint angle pairs of (0.0-19.31 deg), (19.31-20.17 deg), and (20.17-50.93 deg). In the next quarter, we will be testing this method and the tendon excursion method as well as creating the 2D geometric method. We continue to improve image quality with modifications to the hand and wrist holder as well as changes in the image acquisition method.

Progress Report

We are continuing to create methods for measuring tendon moment arm in the MCP joints of the fingers. As described in the previous report, we consider these joints to be simpler than the wrist; hence, we elect to study it first. We use high-resolution, 3D MRI to measure tendon moment arm, and our initial goal is to determine an accurate, practical method. As described in the proposal, we will examine at least 3 methods for analyzing tendon moment arm. They are: tendon excursion, 3D geometric, and 2D geometric. In the previous report, we detailed the tendon excursion method. Presently, we have created an initial version of the 3D geometric method.

Images are acquired with the joint in multiple, fixed rotation angles. Images are acquired with isotropic voxels having 1 mm on a side. Image acquisition is optimized using an MRI T1-weighting so as to have little signal in the absence of water. This gives very dark tendons and bright cancellous bone. The first step is to obtain the axis of rotation of the joint. In order to analyze a joint, from the 3D MRI images, we segment bones on either side of the joint. In the case of the MP joint, these are the 3rd metacarpal and the 3rd proximal phalange. This operation is performed on images in all positions, and the result is given in Figure 1.a.i.1. Currently, this is a laborious, manual step. We hope to improve this to a semi-automated method later. From each bone, we calculate the centroid and 3 principal axes. One can consider the principle axes as giving a reference frame that is anchored to the bone regardless of the orientation of the

bone. This allows us to examine the rotation of the joint and mov ement of the 3rd proximal phalange relative to a fixed frame on the 3rd metacarpal. In addition, we can use the principal axes information to directly calculate the axis of joint rotation using standard mechanics equations (Erdman 1984). Once we determine the axis of rotation, we calculate the tendon moment arm as the minimum distance between the joint axis and the tendon path.

Figure 1.a.i.1 shows segmentations from an analysis of the 3rd MCP joint. Images are acquired at 4 positions including the neutral position. Segmentations and joint center analyses are remarkably consistent. Measured moment arms are 12.45, 14.9, and 13.25 mm for joint angle pairs of (0.0-19.31 deg), (19.31-20.17 deg), and (20.17-50.93 deg). We think that consistency is improved because of the huge redundancy in the measurement. The two bones consist of over 5000 voxels. Errors in a few voxels tend to cancel out. For example, a 5% error might correspond to as many as 250 voxels. We will continue to analyze this and try to determine measurement uncertainties.

We are continuing to improve image quality obtained with the open magnet MRI system. This involves modification of image acquisition parameters as well as improvements to the hand/wrist holder. Since images are obtained over several minutes, we think that images are sometimes degraded due to motion. The improved holder currently under development should improve this situation. In addition, we are now using an coil for imaging the wrist.

Plans for next quarter

As described previously, we have very good first passes on software tools for the tendon excursion method and the 3D geometric method. In the next period, we will create the 2D geometric method. We will also continue experiments aimed at optimizing image quality. We hope to compare all 3 methods on a single subject. In this coming period, we also plan to improve plans for validation.

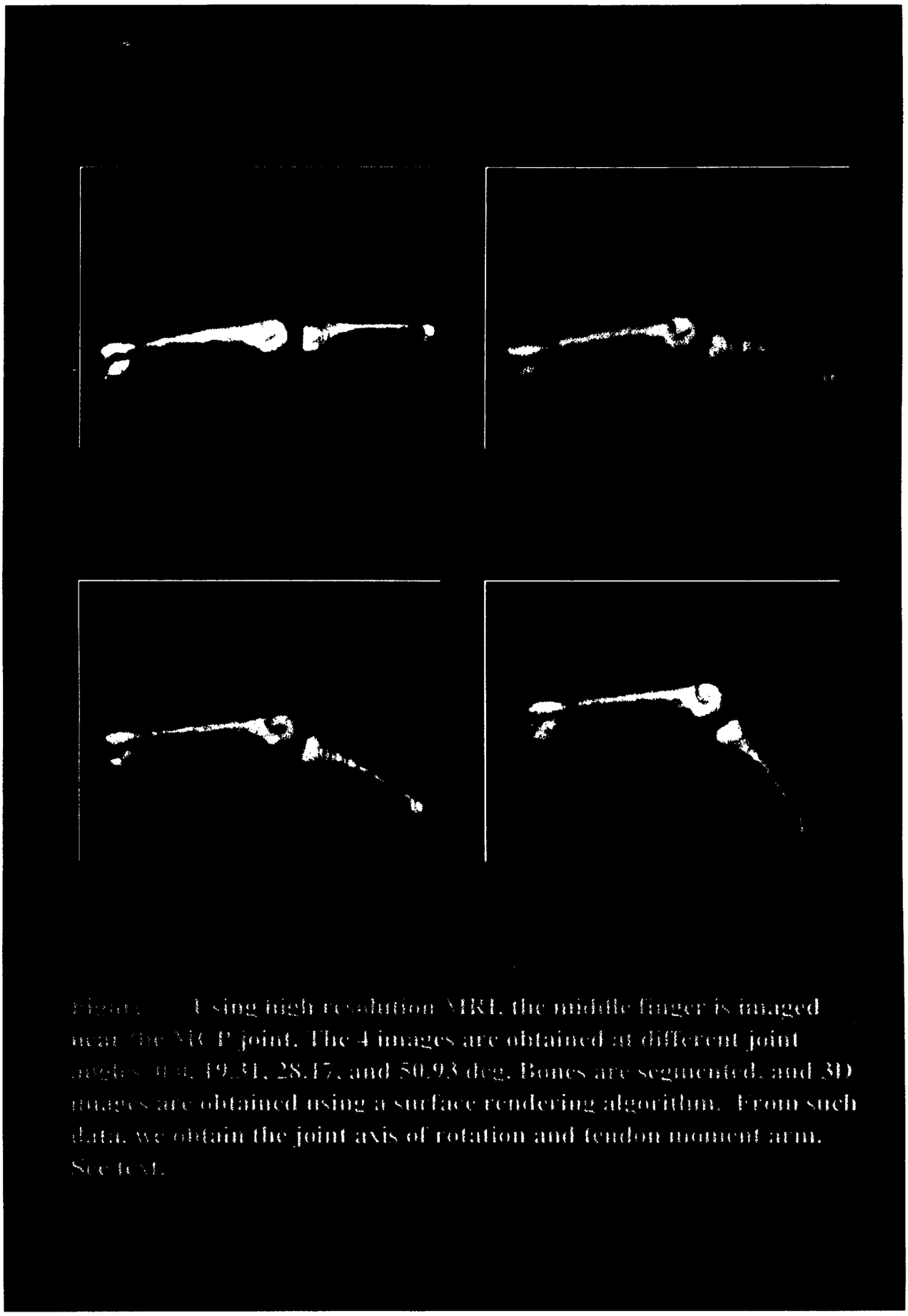

Figure [illegible] Using high resolution MRI, the middle finger is imaged near the MCP joint. The 4 images are obtained at different joint angles: 0.0, 19.31, 28.17, and 50.93 deg. Bones are segmented, and 3D images are obtained using a surface rendering algorithm. From such data, we obtain the joint axis of rotation and tendon moment arm. See text.

1.a.ii. PASSIVE AND ACTIVE MOMENTS

Abstract

During the past quarter, preliminary passive moment measurements were taken on the index finger metacarpophalangeal (MP) joint of both normal and tetraplegic individuals. This data is being used to develop an analysis method for characterizing and comparing one joint's passive properties to another joint's passive properties under the same external conditions.

Purpose

The purpose of this project is to characterize the passive properties of normal and paralyzed hands. This information will be used to determine methods of improving hand grasp and hand posture in FES systems.

Report of Progress

This report has two parts. The first part describes the apparatus used for measuring passive moment. The calibration methods and results are described. The second part presents passive moment data collected from 11 subjects. The issues of measurement repeatability and variability are addressed. Also in this section, data is presented that illustrates the dependence of passive moment on tendon length changes (wrist and proximal interphalangeal joint positions) and shows the relationship between passive moment properties of the MP joints of different digits in the same hand. Finally, parameters for comparing moment-angle curves (MACs) in a quantitative way are presented.

Part 1 - How Measurements Are Made

Overview

Passive moment measurements are made by rotating a finger joint through its range while measuring the joint angle and the resistance to rotation simultaneously.

Figure 1.a.ii.1 is a diagram of the apparatus. The subject's forearm is placed in a padded forearm support (A) and is secured comfortably with velcro straps. The hand is placed into the hand holder (B) which also serves as a wrist splint. The hand holder can be rotated and pinned in 20° increments, thereby positioning the wrist at different angles. Of the three joints in the finger to be tested, two are splinted into a desired fixed position with a finger splint. The free joint is rotated through its range and is aligned by eye with the apparatus' motor-driven shaft (C). A rod extends from the finger splint and inserts into one of the holes of the force transducer beam (D). This beam is attached to a horizontal arm (E) which is rotated about the shaft driven by a gear-head motor (F). The speed of rotation is set and maintained by an electronic controller. The strain gages mounted on the force transducer record the shear force in the beam during the finger motion. A potentiometer (G) attached to the rotating shaft is used to record the joint angle. A circular plexiglas protractor (H) is used to calibrate the potentiometer. The range through which each joint is rotated is set by mounting limit switches (I) to the protractor so that they contact the swinging horizontal arm when the extension and flexion extremes are reached. When the arm closes either switch, the motor reverses its direction of rotation. Extension and flexion extremes are determined to be the joint angle at which the resistance moment is about 40 N·cm. Because of the great importance of aligning the motor-driven shaft with the joint's axis of rotation, the apparatus was designed to move relative to the joint, thereby allowing the investigator to align the apparatus to the joint over a wide range of joint locations.

Once the subject and limit switches have been positioned, passive moment measurements are taken. The motor is turned on and set at a rate which causes a joint rotation of 50 degrees per second. After a sufficient number of warm-up cycles (see *Effect of Preconditioning the Joint* below), the transducers are sampled at 100 Hz for one cycle or for a number of cycles of joint rotation. A cycle begins when the joint is in its midrange and being extended. A complete cycle consists of joint rotation from near its rest position to its maximum extension, reversal of joint rotation to maximum flexion, and return of the

The gear motor is a 115 V, DC, 1/50 hp, 29 rpm motor (Bodine Electric Co.). The motor is controlled by an electronic controller which maintains the speed of rotation. By adjusting the speed knob on the front panel, the angular rotation of a finger joint can be varied between 7.2 and 57.7 degrees per second (0.126 to 1.007 rad/s). The front panel also includes an on/off switch, forward and reverse switches, and a kill switch.

Data Acquisition

The data acquired from each trial consists of moment, angle, time, and angular velocity (time derivative of angle). Using Labview® software, a virtual instrument (VI) was created to acquire the data. The strain gages and potentiometer are sampled simultaneously at a rate of 100 Hz. Charts of passive moment versus time, joint angle versus time, angular velocity versus time, and passive moment versus joint angle are generated as the data is sampled.

Part 2 - Preliminary Measurements

Preliminary measurements of passive moments have been used for the following purposes: 1) to assess the effect of preconditioning the joint, 2) to determine the repeatability of the measurement, 3) to examine the variability of the passive moment over a period of weeks, 4) to investigate the sensitivity of the measurement to misalignment of the apparatus to the joint, 5) to investigate the effect of wrist and interphalangeal joint positions on the moment-angle curve (MAC) of the index MP joint, 6) to examine the differences in moment-angle curves generated by the MP joints of the different fingers of the same hand, and 7) to develop quantitative methods for comparing MACs generated by different joints and generated by the same joint under different conditions.

The index MP joints of eight normals and three tetraplegic individuals were tested under conditions that varied according to the purpose of the test.

Effect of Preconditioning the Joint

It was observed that the first MACs acquired are different from MACs measured once the joint has been ranged a number of times. Figure 1.a.ii.3 shows the passive moment over time as the joint is cycled through its range 15 times. The dotted trace shows the passive moment measured without stretching the joint prior to testing. The solid trace shows the passive moment of the same joint ten minutes after the first measurement was taken. Notice that the peak moments at the extremes of flexion and extension in the dotted trace level out after only 2 cycles. The solid trace shows that after 10 minutes of the joint resting in its neutral position following the previous 15 cycles of ranging the peak passive moments remained at the level they had settled to in the previous measurement. That is, the preconditioning effect had not worn off after 10 minutes. The number of cycles it takes before the passive moments stabilize probably depends on the passive properties of the joint itself, but to be safe, subsequent passive moment measurements were made after the joint had been cycled through its range at least 5 times.

Repeatability

Two repeatability tests were performed on the same MP joint. The first test measured the consistency of the measurement when the hand is not removed from the apparatus between measurements. The second test gave a measure of repeatability when the hand is removed from the apparatus and then remounted between each measurement. In each of the two tests, five MACs were acquired and a curve was fit to each MAC yielding four parameters per MAC (see *Comparing MACs* below). Then coefficients of variation were calculated for each curve parameter. Figure 1.a.ii.4 shows the five MACs generated without removing the hand from the apparatus and Figure 1.a.ii.5 shows the five MACs measured when the hand was removed and remounted between measurements. Coefficients of variation ranged from 0.7% to 8.8% in the test where the hand was not removed from the apparatus and ranged from 3.5% to 13.7% in the test when the hand was removed and remounted between measurements.

Variability of Passive Moment Over Time

One subject's joint was tested at random times over a period of 5 weeks. These moment-angle curves are shown in Figure 1.a.ii.6. Using the same method of analysis as in the repeatability tests, the coefficients of variation for the parameters resulting from curve fits ranged from 8.2% to 39.4%.

Alignment Effects

We investigated how sensitive the moment-angle curves are to misalignment of the joint to the motor-driven shaft. First a MAC was acquired with the MP joint lined up by eye as accurately possible. In the following trials passive moments were measured with the shaft displaced up to 0.5 inch dorsally, volarly, distally, and proximally from the initial position. The results indicate that the MACs are more sensitive to a proximal-distal misalignment than to a dorsal-volar misalignment. Misalignments of 0.5 inches resulted in passive moments that differed in magnitude by as much as 50% at the extremes of joint rotation. However, as the repeatability experiment in which the hand was removed and remounted between measurements showed, misalignments of this magnitude are not expected.

Effect of Wrist Position

The MP passive moments were measured with the wrist fixed at different angles while the index proximal and distal interphalangeal joints were splinted straight. This testing was done with five normal and two tetraplegic subjects. Figure 1.a.ii.7 shows three moment-angle curves generated by the index finger's MP joint of a normal subject. Each MAC corresponds to a different wrist position. The MAC shifted farthest to the right of the figure was generated with the wrist at 60° of extension, while the curve at the left of the figure was generated when the wrist was flexed 80°. These curves show that wrist extension limits MP extension but promotes MP flexion while wrist flexion has the opposite effect. This observation was true for all the subjects tested.

One subject's MP was tested while the wrist was fixed in three different positions. For each position of wrist fixation, the subject's proximal interphalangeal (PIP) joint was also fixed in three different positions. This data is shown in Figure 1.a.ii.8. In this subject, for each wrist position it appears that greater PIP flexion shifts the curves toward greater extension. This makes sense because, like wrist flexion, PIP flexion tightens extensors and loosens flexors, making MP extension easier and MP flexion more difficult. However, with an extended wrist, PIP position had much less effect on MP mobility than when the wrist was flexed.

Different Fingers of the Same Hand

The apparatus allows measurement of the passive moments in the MP joints of all four fingers. Figure 1.a.ii.9 shows the MACs of the MP joints of each finger of the hand. One other subject was tested in the same way.

Comparing MACs

In order to compare one moment-angle curve with another, the MACs can be plotted on the same page and the differences can be observed. Figure 1.a.ii.10 shows the MACs measured from six subjects under the same conditions: the wrist, PIP, and DIP were splinted straight. Just by observation you can see differences in passive range of motion and joint stiffness across subjects. However, quantitative comparisons must be made. A first step toward this goal is to fit a curve to each MAC. A function described by the equation, $M = a(e^{b(\emptyset-\emptyset r)} - e^{c(\emptyset-\emptyset r)})$ nicely fits the moment-angle curves data. Figure 1.a.ii.11 shows an example of passive moment date with a curve fit. Each curve fit yields four parameters: a, b, c, and Ør. Parameter a determines how wide the "flat" region of the curve stretches, b is a measure of the slope of the extension side of the curve, c is a measure of the slope of the flexion side of the curve, and Ør is the angle at which the curve fit crosses the abscissa (where passive moment is zero). The Ør parameter

is a measure of the angle at which the joint rests when the wrist is in the position tested. It is difficult to compare parameters a, b, and c from one MAC to another because they depend on each other. That is, parameter b could have the same value in different curves, but the extension slopes would look very different if parameter a and Ør were not also the same between curves. In order to make meaningful comparisons between MACs, the four curve fit parameters were used to compute five other curve features as shown in Figure 1.a.ii.11. Four of these features are slopes of line segments connecting specific points on the fitted curve. The segment that connects the point on the curve that crosses zero moment to the point on the curve that crosses 20 N·cm defines a slope labeled Ext(0-20). Flx(0-20) is defined by a segment connecting points where the curve crosses 0 and -20 N·cm. Ext(20-30) is defined by the segment connecting points where the curve crosses 20 and 30 N·cm while Flx(20-30) is the slope of a segment that connects the curve intersections of -20 and -30 N·cm. These four parameters are indications of the stiffness of the joint in its midrange and at its extremes. Additionally, a measure of passive range of motion (PROM) can be computed as the joint range between 20 and -20 N·cm as shown in Figure 1.a.ii.11. These parameters can be directly compared across subjects.

Four normal and two tetraplegic index finger MP joints were tested under two conditions of the wrist splinted at 0° and then 60° of extension. For each subject the four stiffness parameters (Ext(0-20), Ext(20-30), Flx(0-20), Flx(20-30)) as well as Ør and PROM were computed for each wrist condition. Figure 1.a.ii.12 shows the four stiffness parameters for each subject when the wrist was at 0°. Figure 1.a.ii.13 shows the four stiffness parameters for each subject when the wrist was at 60° of extension. In both figures the "Flx" parameters are greater than the "Ext" parameters; however the difference between the Flx and Ext parameters are greater with the wrist extended than with the wrist straight. Figure 1.a.ii.14 shows the change in each stiffness parameter for each subject as their wrist was extended from 0° to 60°. The two tetraplegic subjects have an asterisk by their initials. Overall it appears that the two tetraplegic joints undergo greater stiffness changes as the wrist is extended than the joints of normal hands.

For the same six subjects, PROM and Ør were computed and compared at the two wrist positions. Figure 1.a.ii.15 shows the PROM and Ør for each subject when the wrist was at 0° and Figure 1.a.ii.16 shows the PROM and Ør for each subject when the wrist was at 60° of extension. In both figures it appears that the two tetraplegic subjects have less PROM in the MP flexion direction than the normals have. Figure 1.a.ii.17 shows the change in PROM and Ør for each subject as their wrist was extended from 0° to 60°. Here it is apparent that the PROM decreased much more for the tetraplegic joints than for the normal joints as the wrist extended from 0° to 60°.

The four curve parameters, a, b, c, and Ør can also be used to compute the derivative of the fitted curve. The derivative of the fitted curve corresponds to the stiffness of the joint through its range of motion. Figure 1.a.ii.18 shows the derivative of the fitted curves of different subjects whose wrists were fixed at 0°.

Plans for Next Quarter

More data will be collected and analyzed in the next quarter. Specifically, MP data at different wrist angles will be collected from more subjects. Analysis of this data should reveal trends and differences between tetraplegic and normal subjects. A sensitivity analysis of the derived parameters will be done. Also EMGs will be monitored during some passive moment testing to verify passivity.

Reference

Esteki, A. and Mansour, J. M. (1996) An experimentally based nonlinear viscoelastic model of joint passive moment. *J. Biomechanics* 29, 443-450.

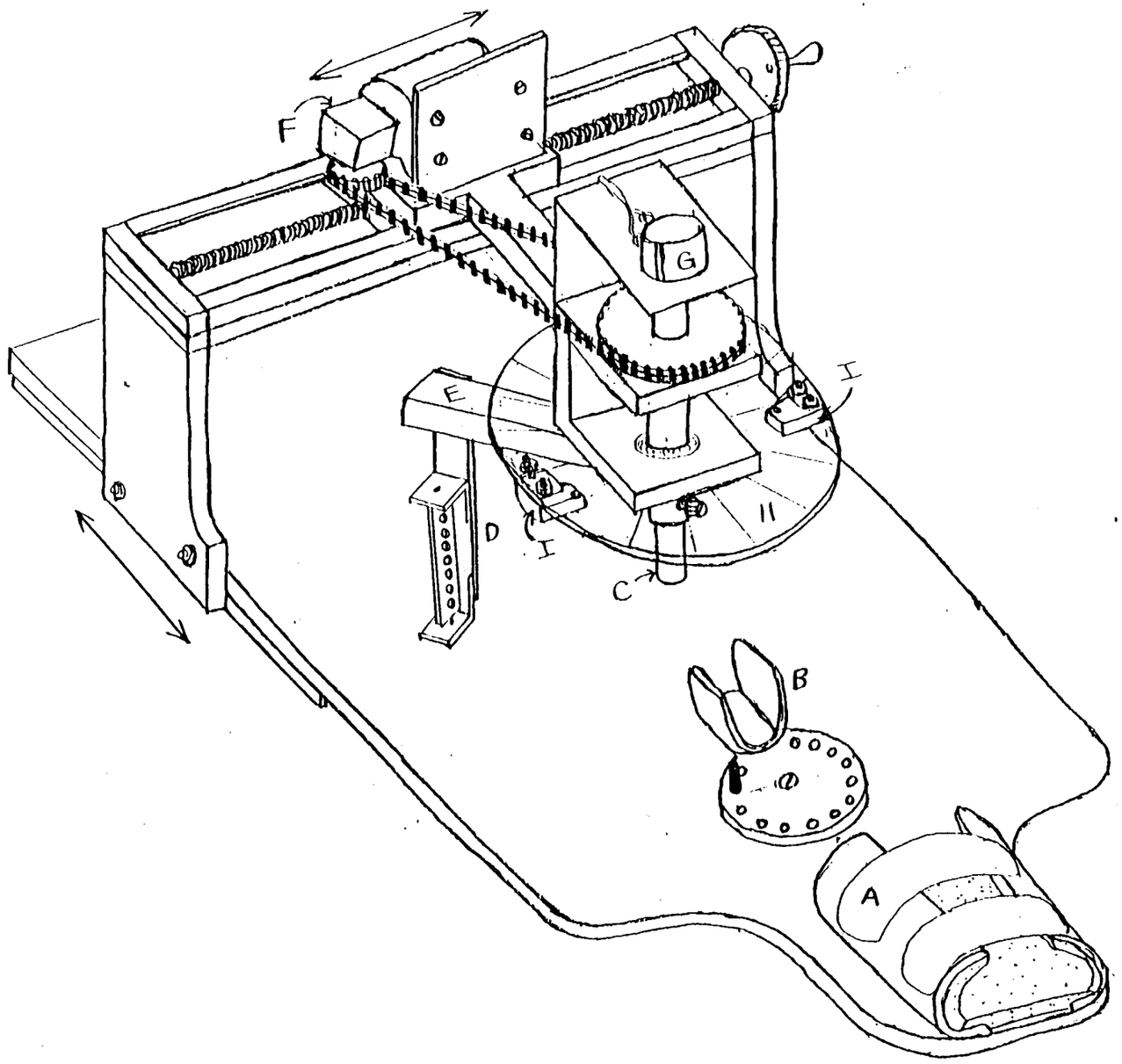

Figure 1.a.ii.1. Apparatus for measuring the passive moment about the finger joints.

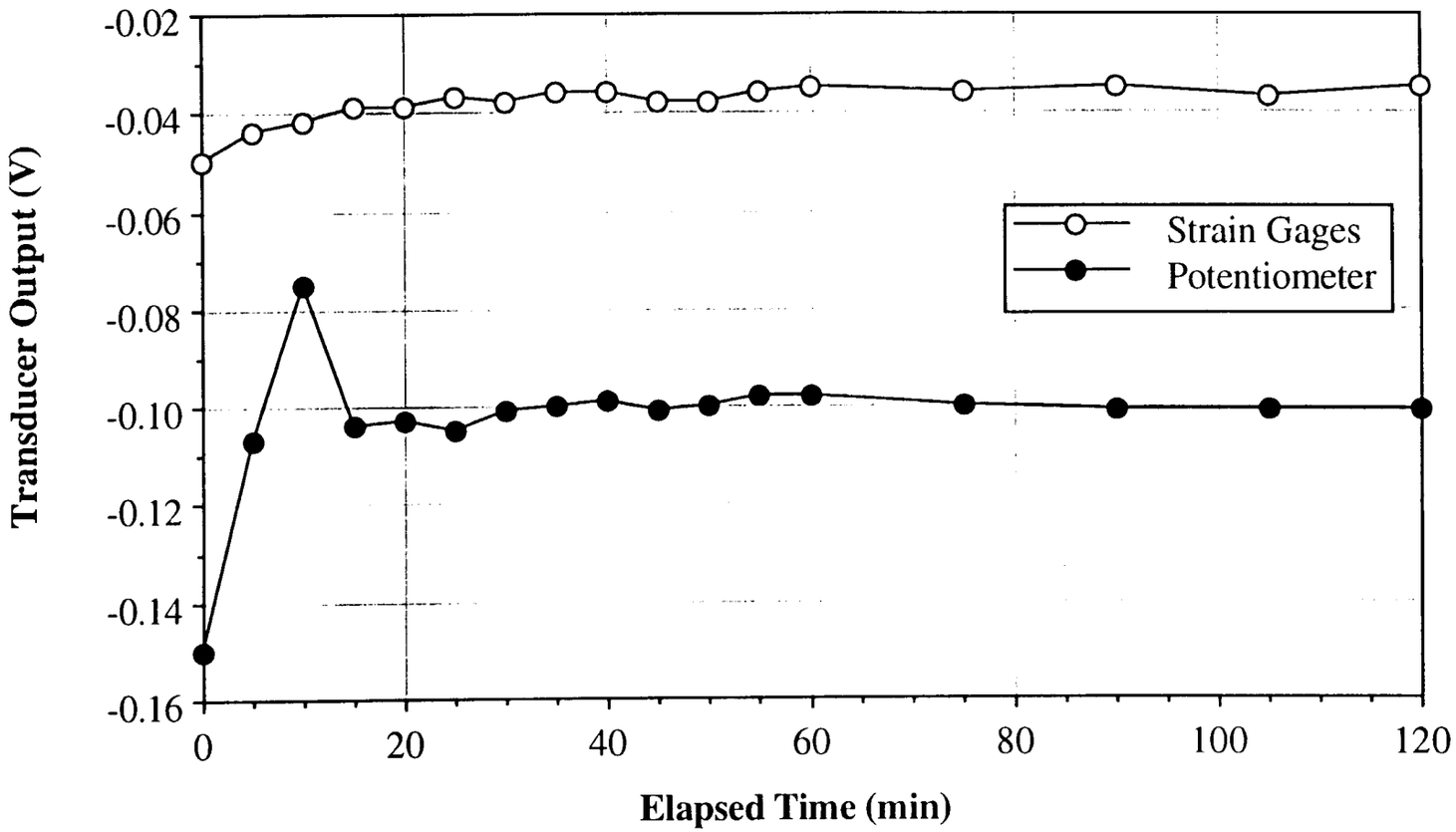

Figure 1.a.ii.2. Voltage drift in the force and angle transducer signals. Time starts the moment the signal amplifier is turned on.

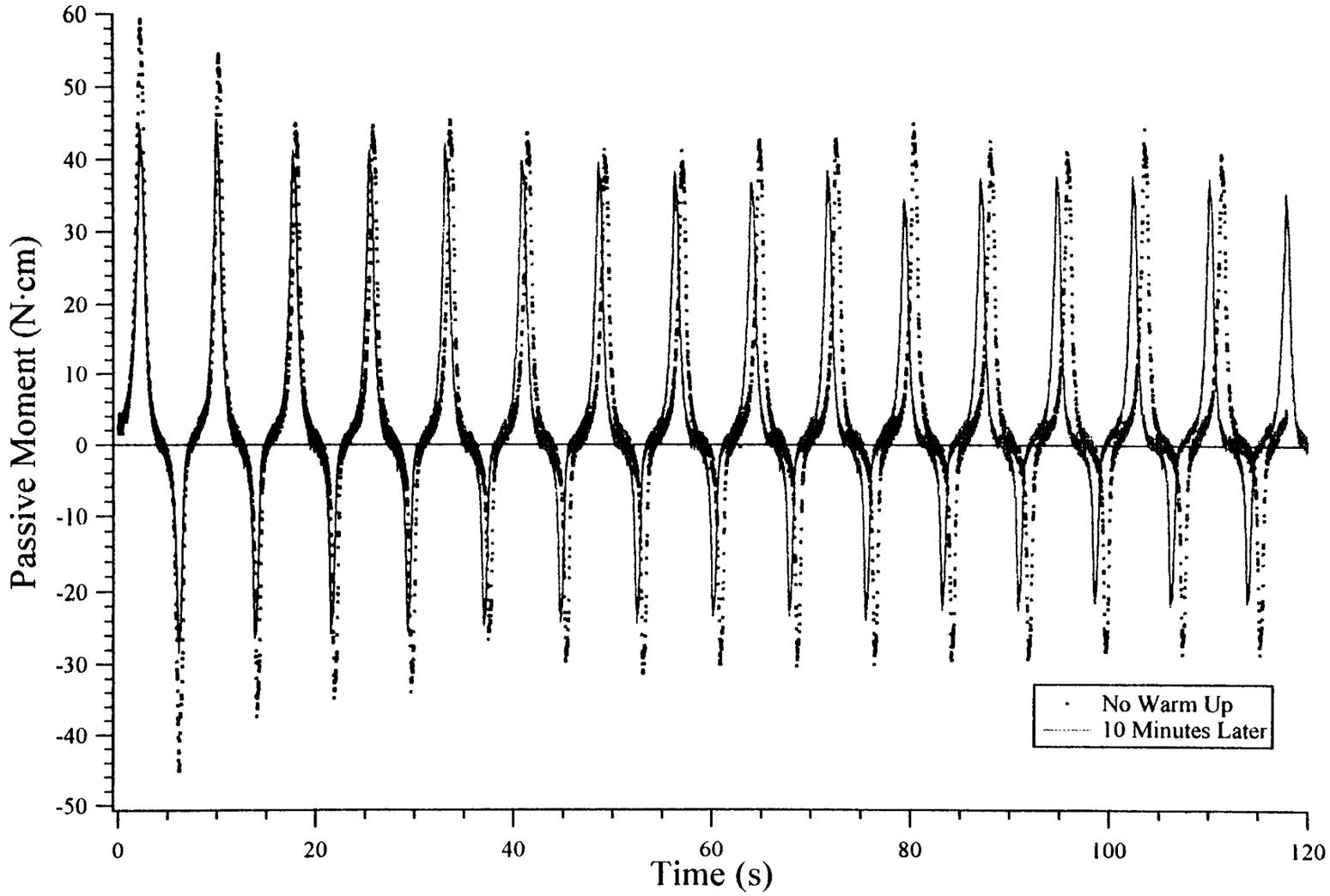

Figure 1.a.ii.3. Passive moment during 15 cycles of joint rotation. The dotted line is the passive moment measured with no stretching of the joint prior to the measurement. The solid line is the passive moment measured ten minutes after the first measurement was completed.

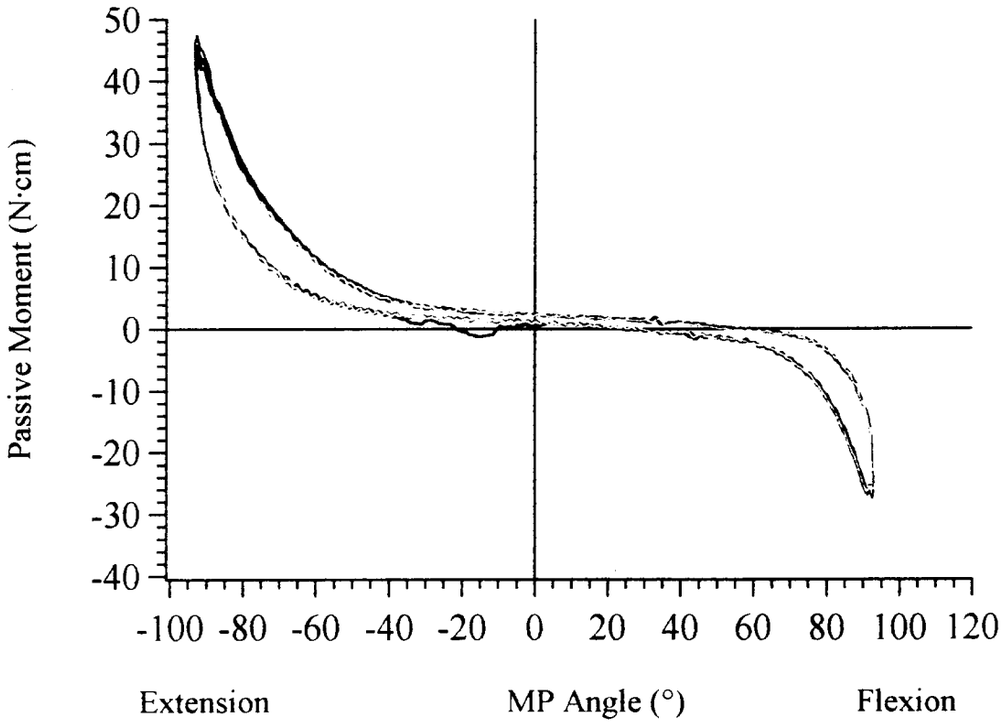

Figure 1.a.ii.4. Five separate MP joint moment-angle curves measured consecutively without removing the subject's hand from the apparatus between measurements.

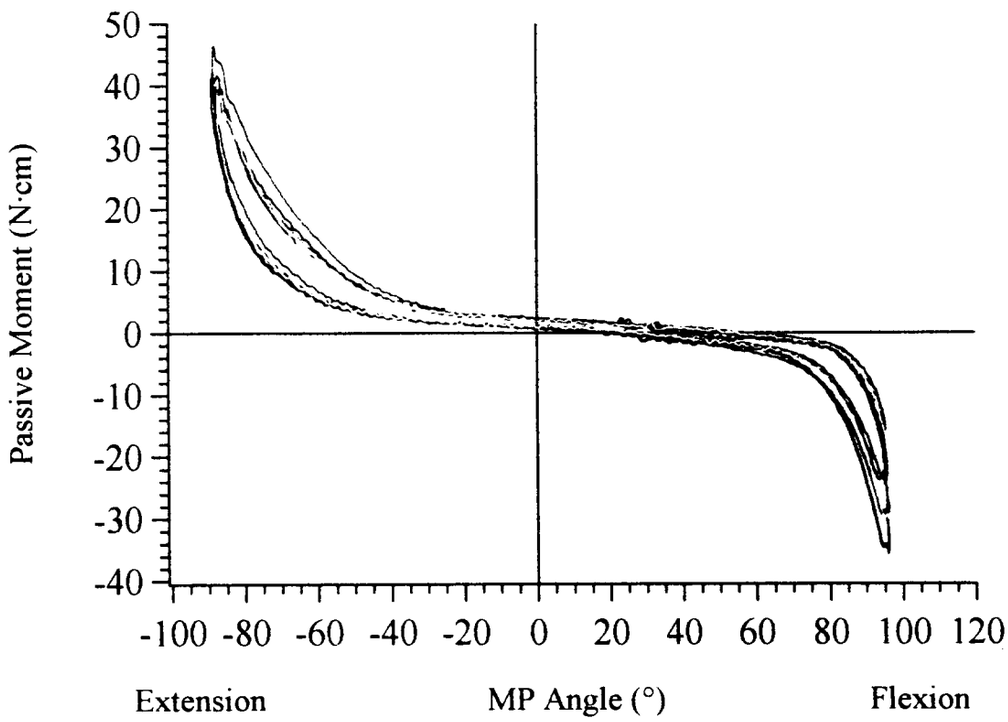

Figure 1.a.ii.5. Five separate MP joint moment-angle curves. Between each measurement the hand was removed from the apparatus and then remounted.

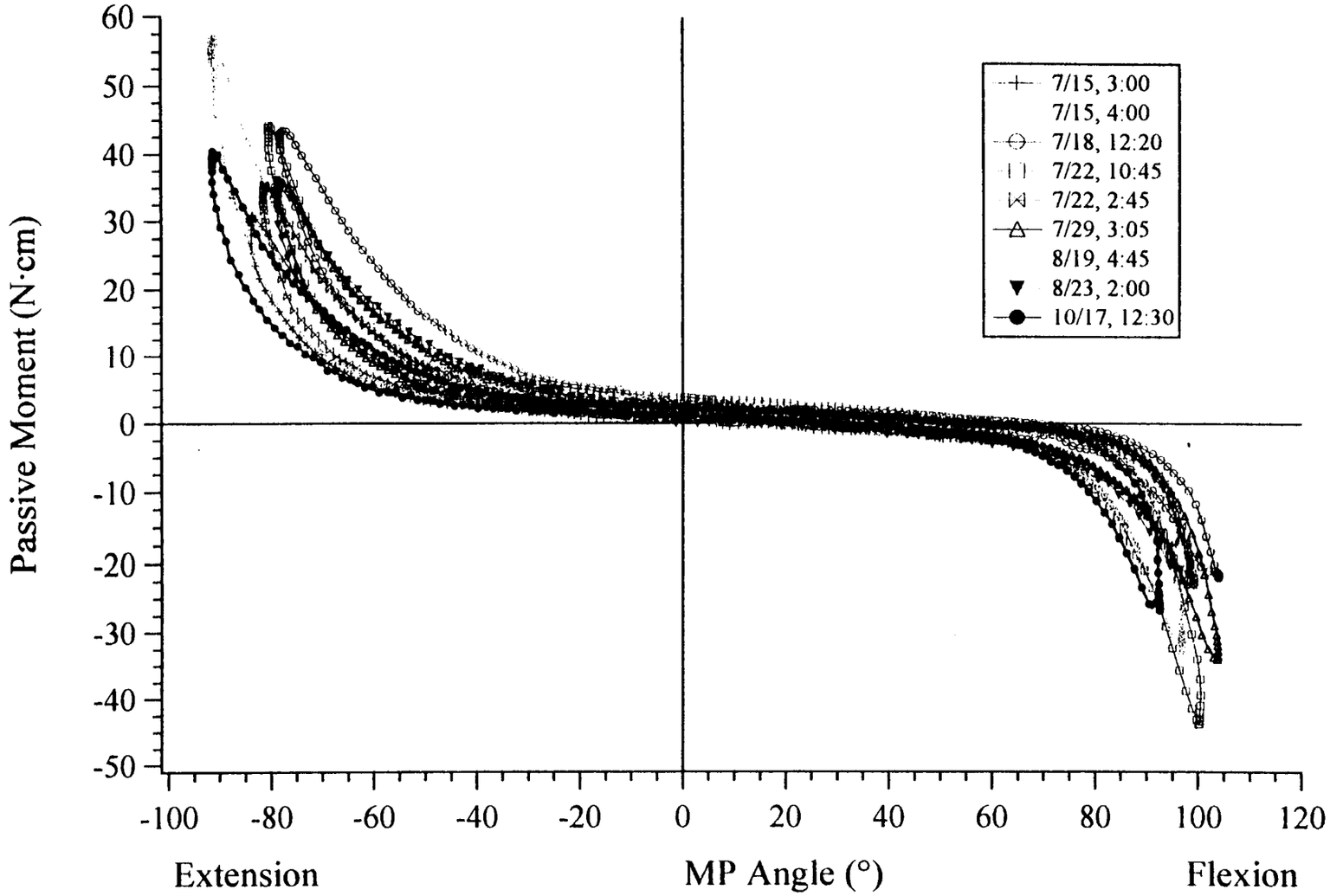

Figure 1.a.ii.6. Moment-angle curves measured from the same joint under the same external conditions at random times over a period of five weeks show the variability of the passive moment within a single subject.

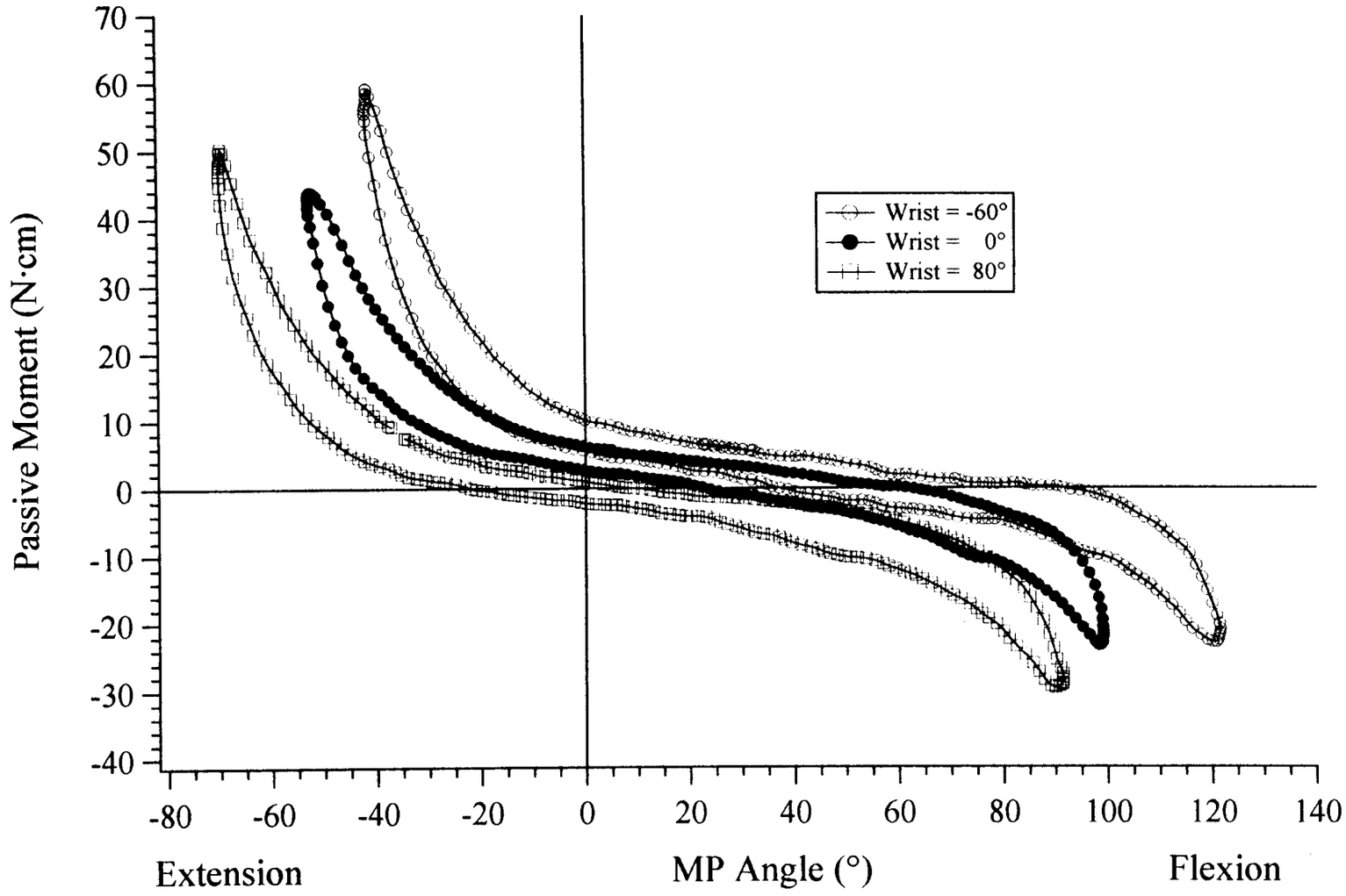

Figure 1.a.ii.7. Moment-angle curve measured from the same joint with the wrist fixed in three different positions show how the passive moment depends on wrist position.

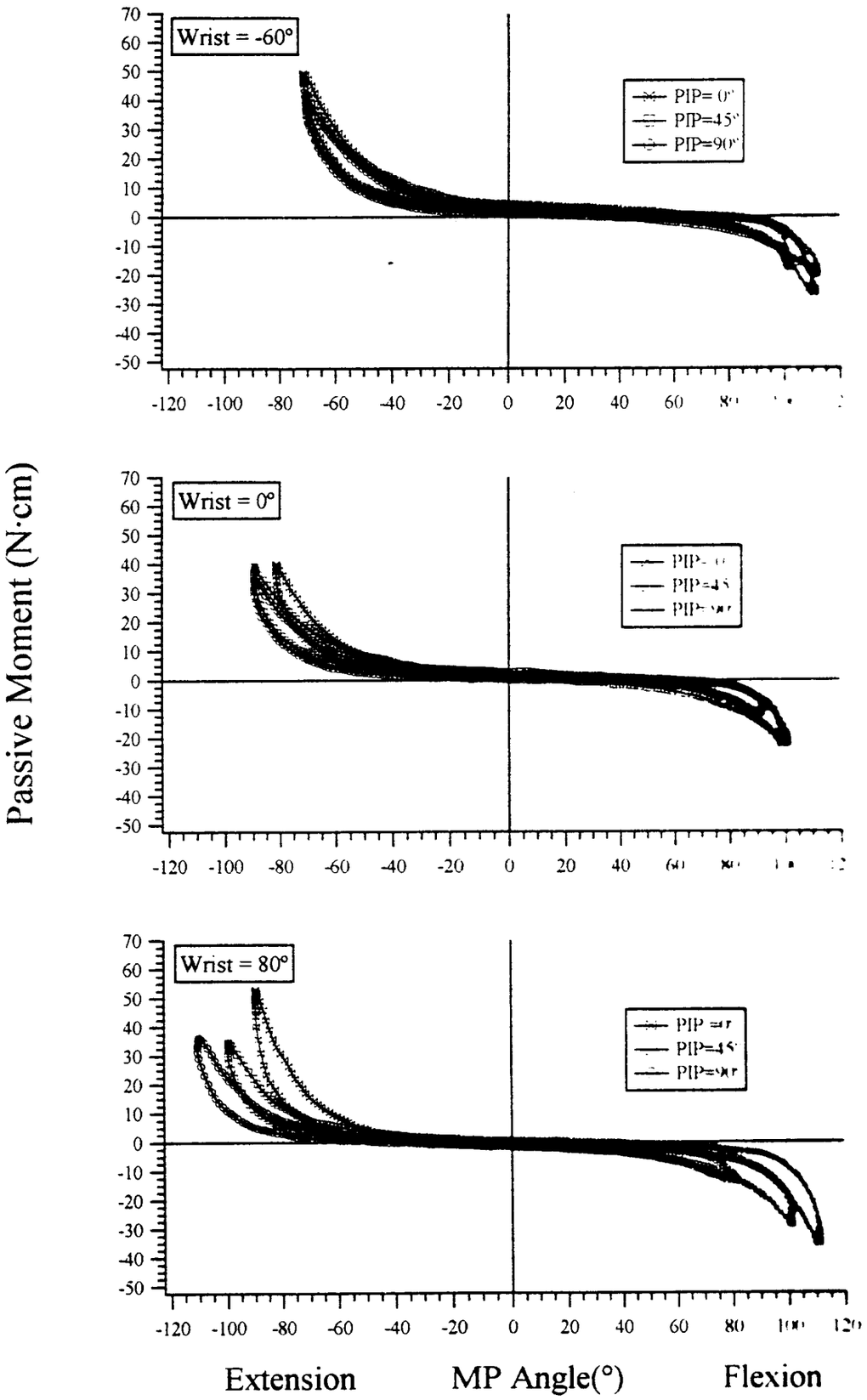

Figure 1.a.ii.8. Moment-angle curves measured at three wrist positions. At each wrist position, the PIP joint was also fixed in three different positions.

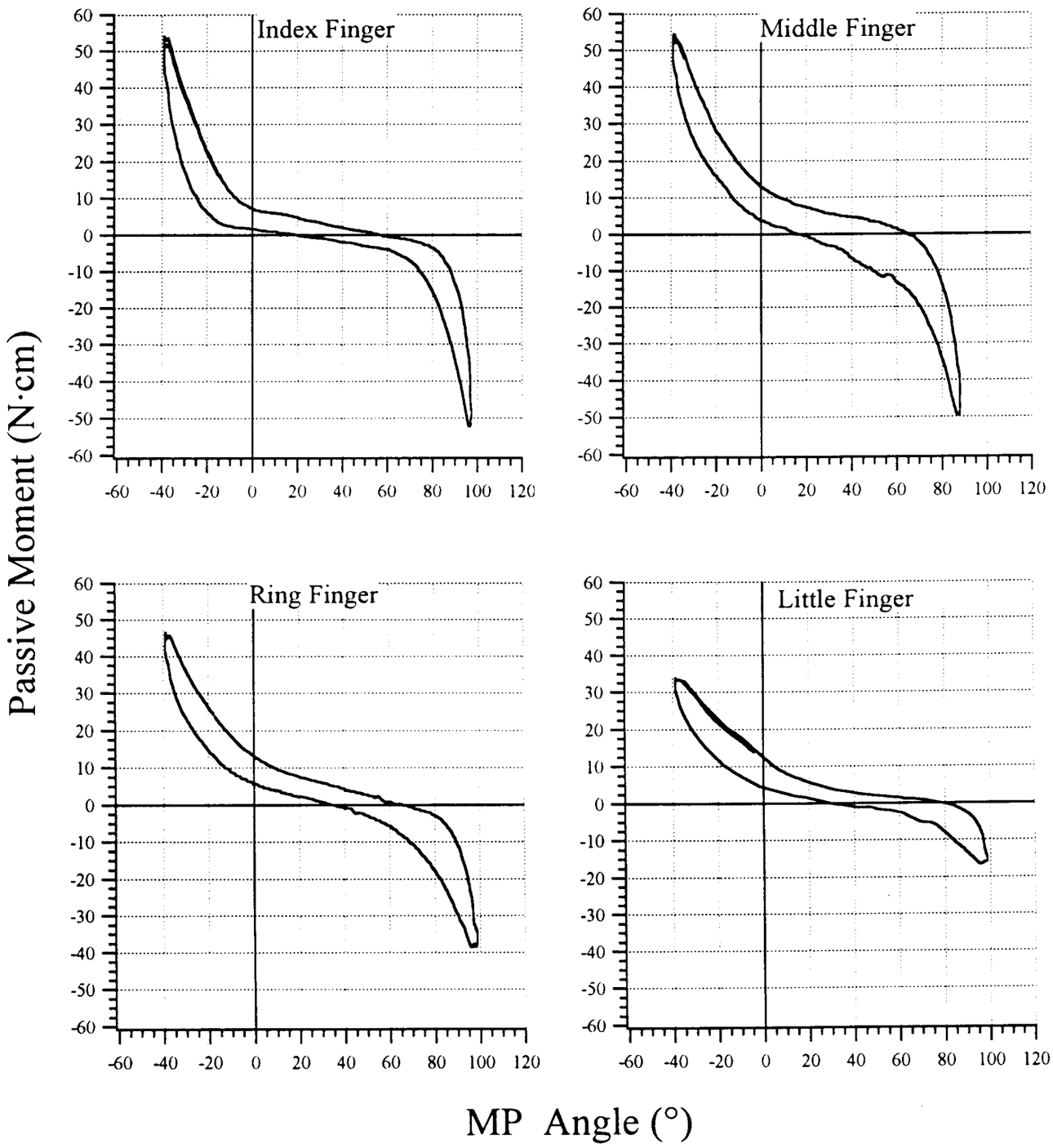

Figure 1.a.ii.9. Moment-angle curves from each MP joint of the four digits of the same hand.

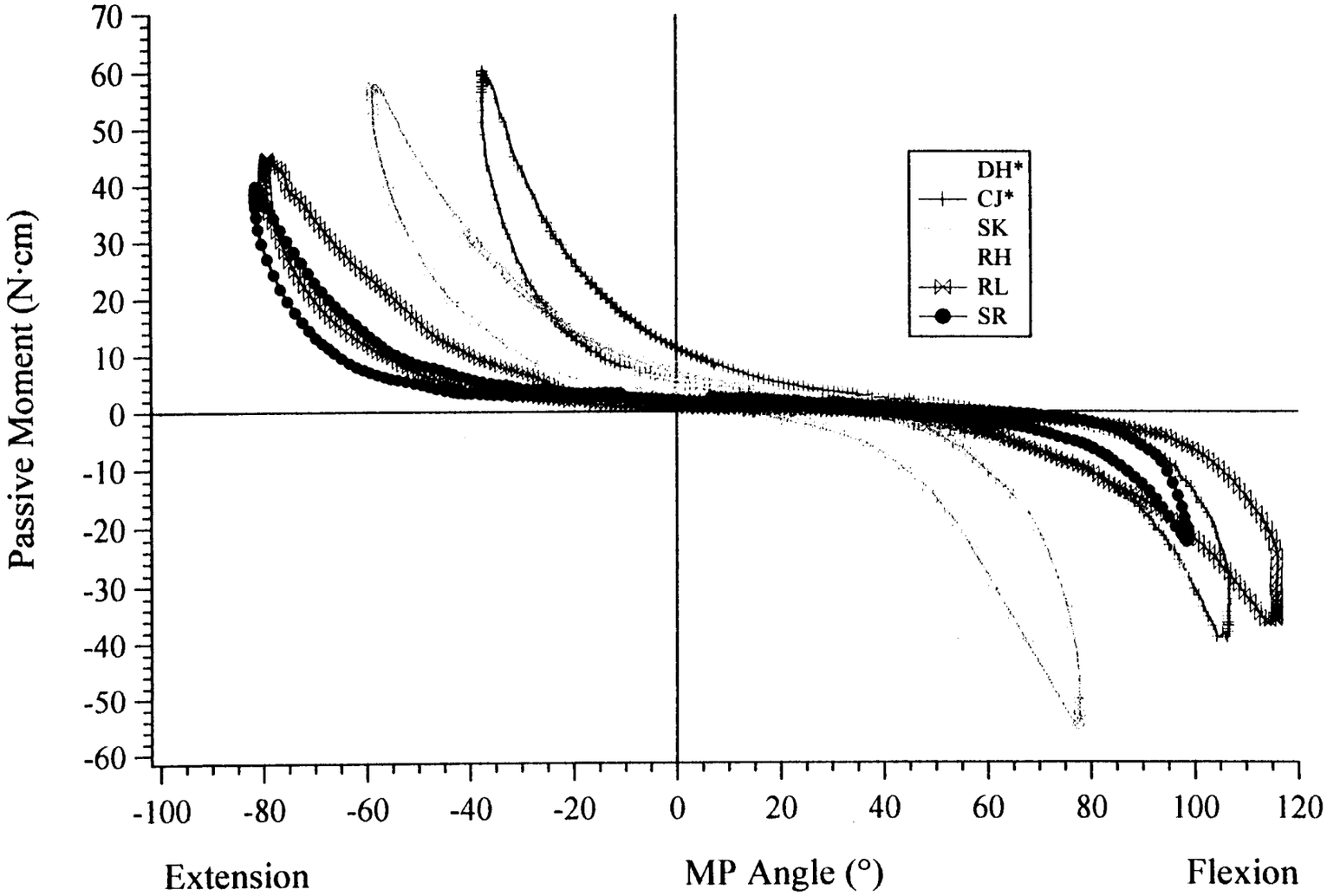

Figure 1.a.ii.10. Moment-angle curves measured from six subjects under the same external conditions show the variability of the passive moment across subjects. Subjects with an asterisk beside their initials are tetraplegic.

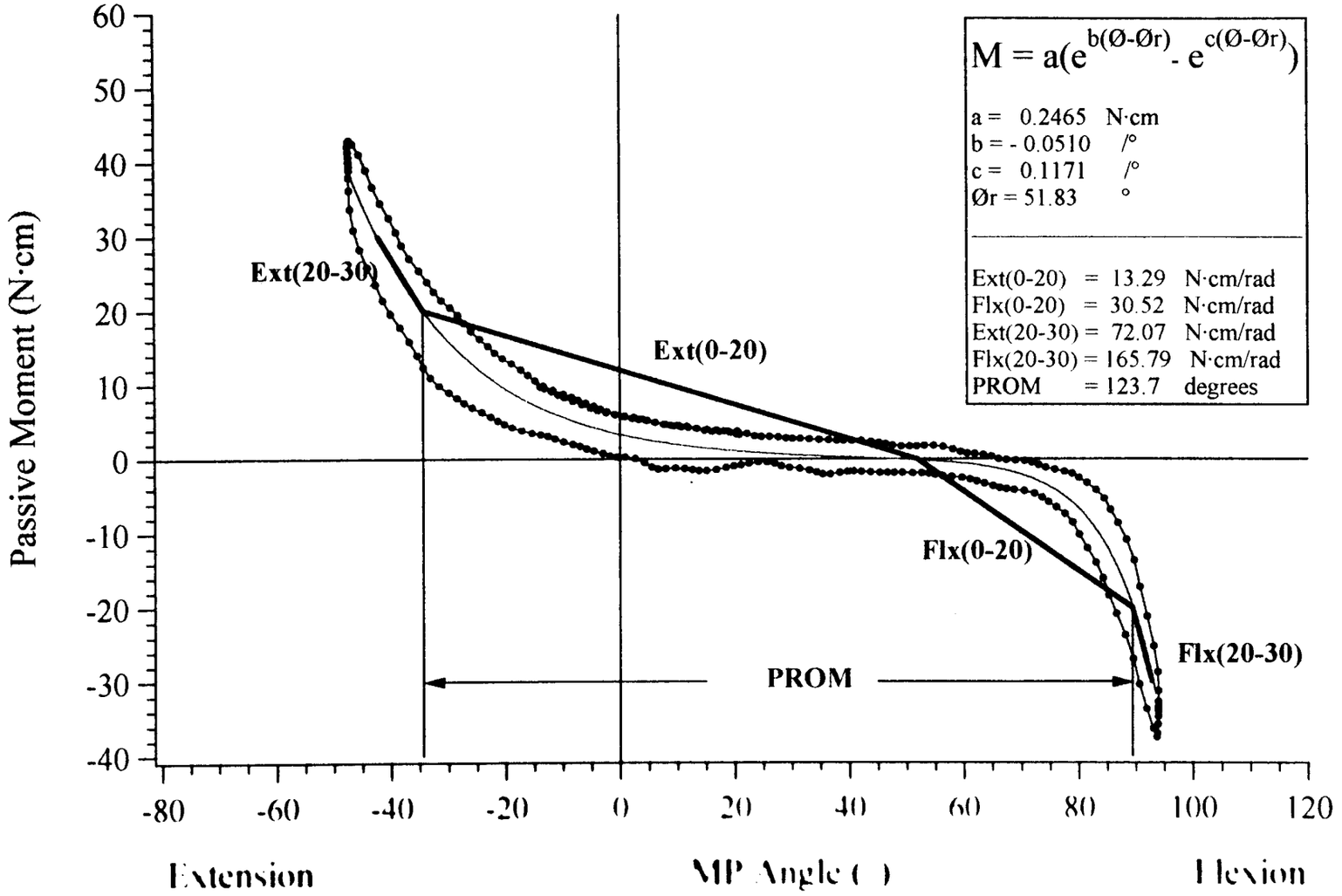

Figure 1.a.ii.11. Example moment-angle curve with curve fit, curve fit parameters, and parameters derived from the curve fit parameters.

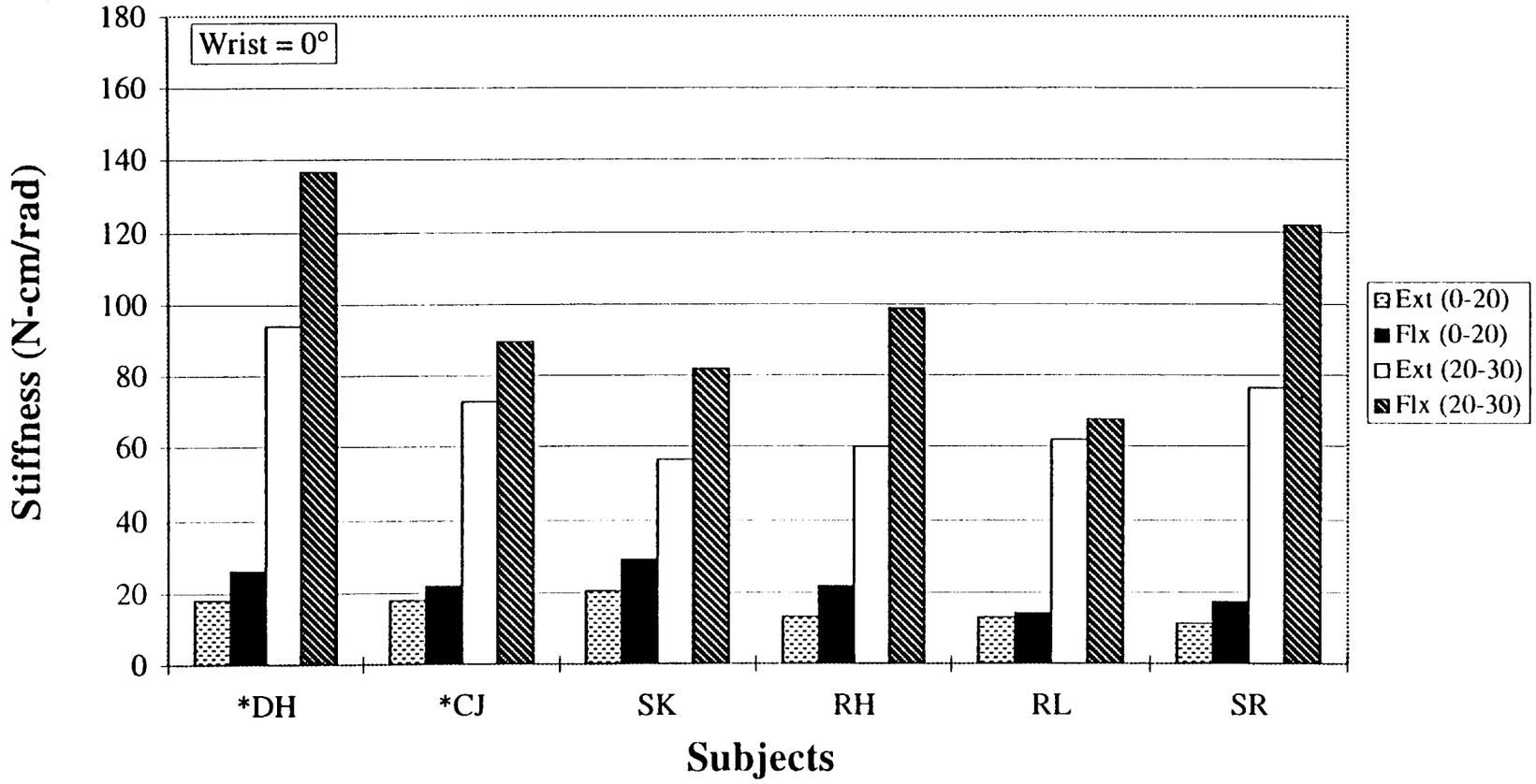

Figure 1.a.ii.12. Four stiffness parameters computed for each subject for the case when the wrist was fixed at 0°. The subjects with an asterisk beside their initials are tetraplegic.

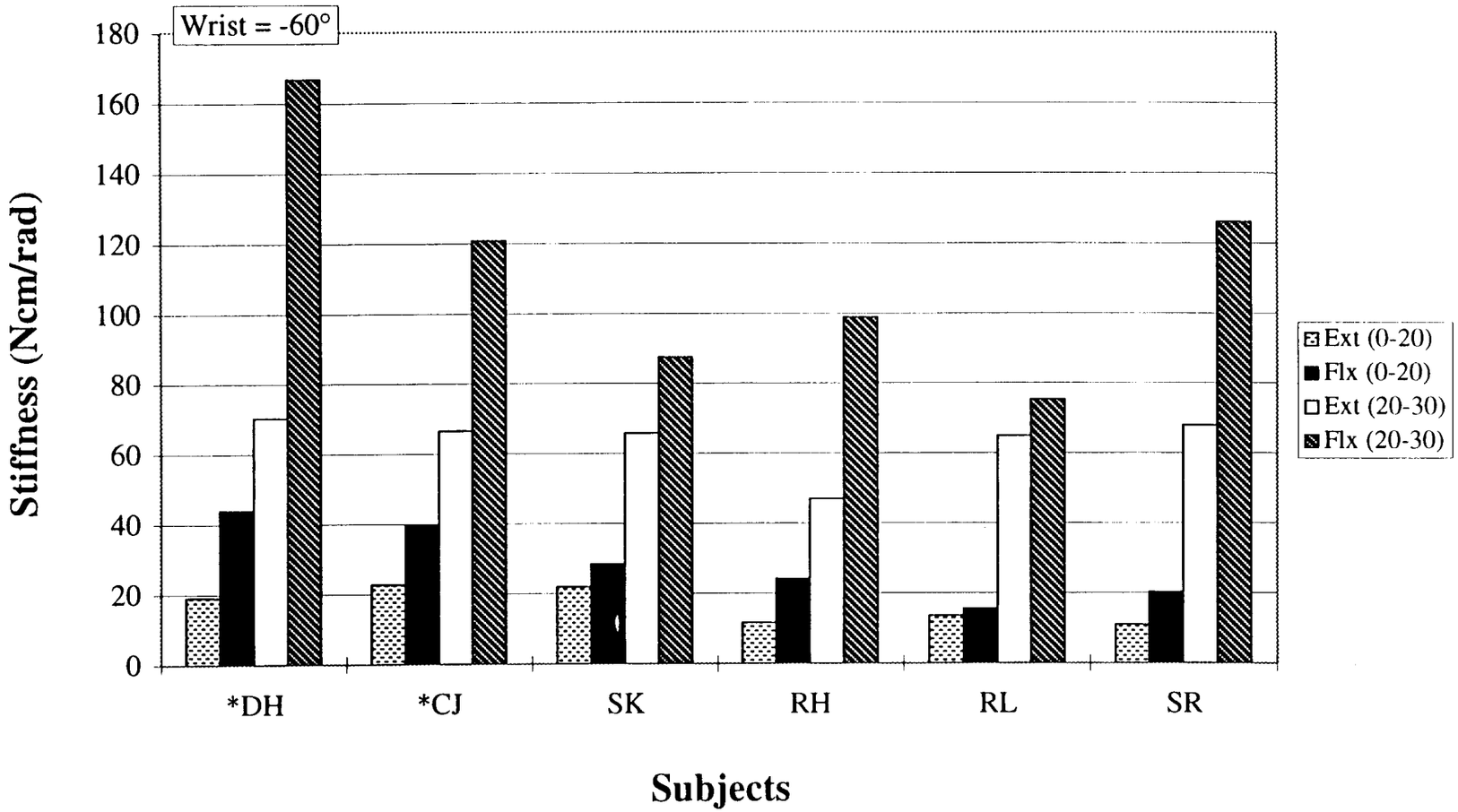

Figure 1.a.ii.13. Four stiffness parameters computed for each subject for the case when the wrist was fixed at 60° of extension. The subjects with an asterisk beside their initials are tetraplegic.

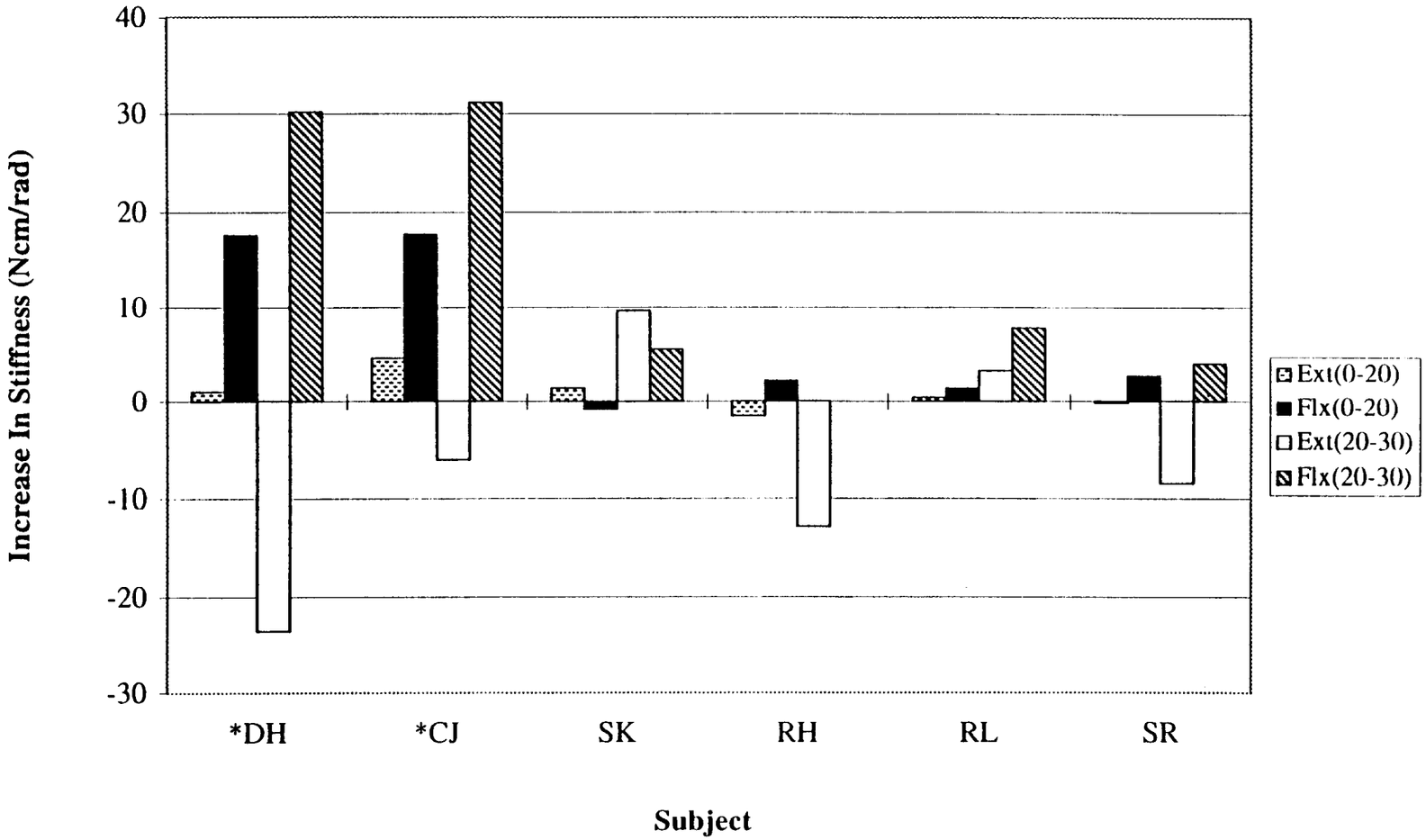

Figure 1.a.ii.14. The change in each stiffness parameter for each subject as the wrist extends from 0° to 60°. The subjects with an asterisk beside their initials are tetraplegic.

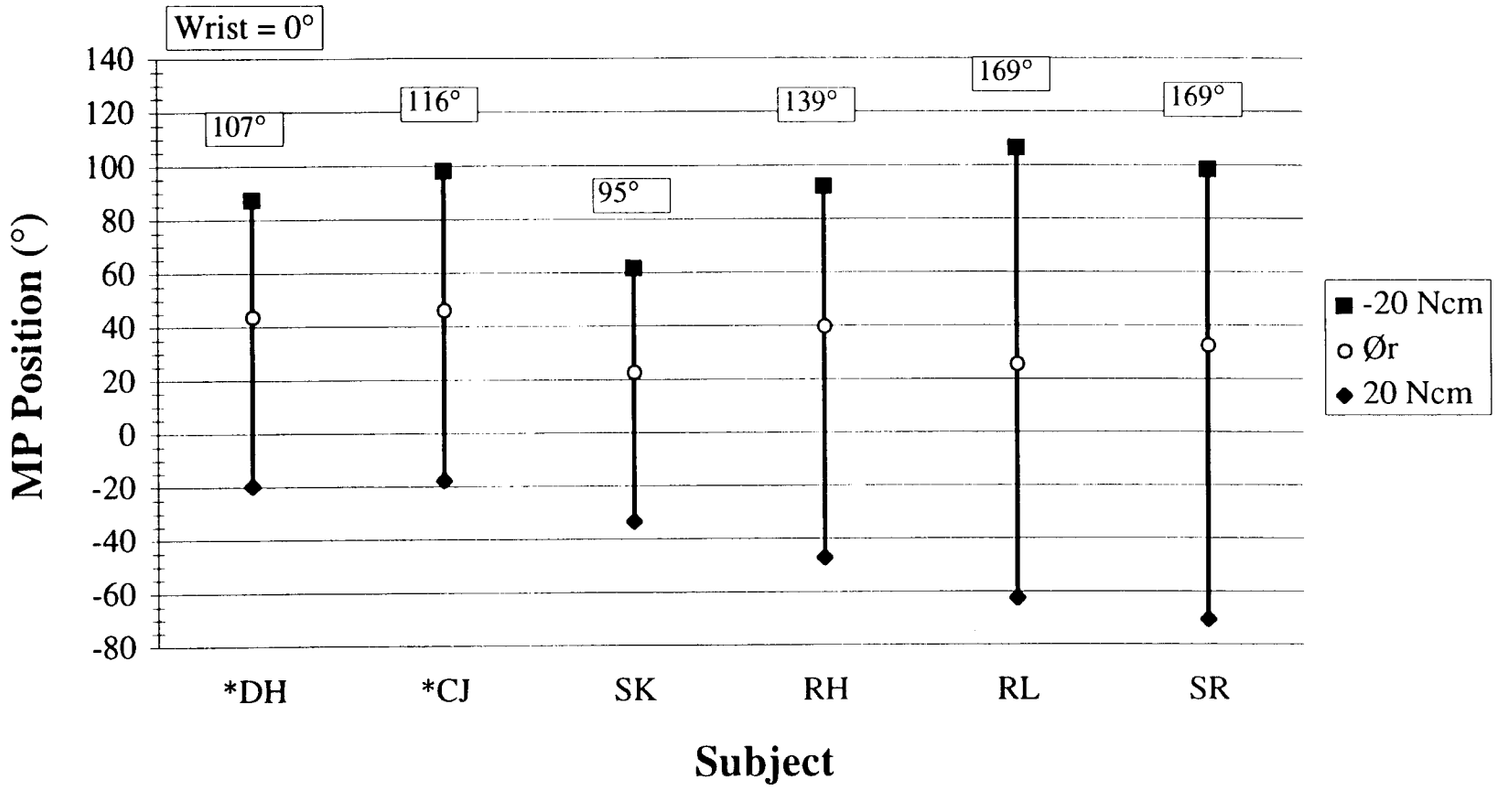

Figure 1.a.ii.15. PROM and Ør computed for each subject for the case when the wrist was fixed at 0°. Subjects with an asterisk beside their initials are tetraplegic. The boxed values are the MP PROM between -20 and 20 N·cm.

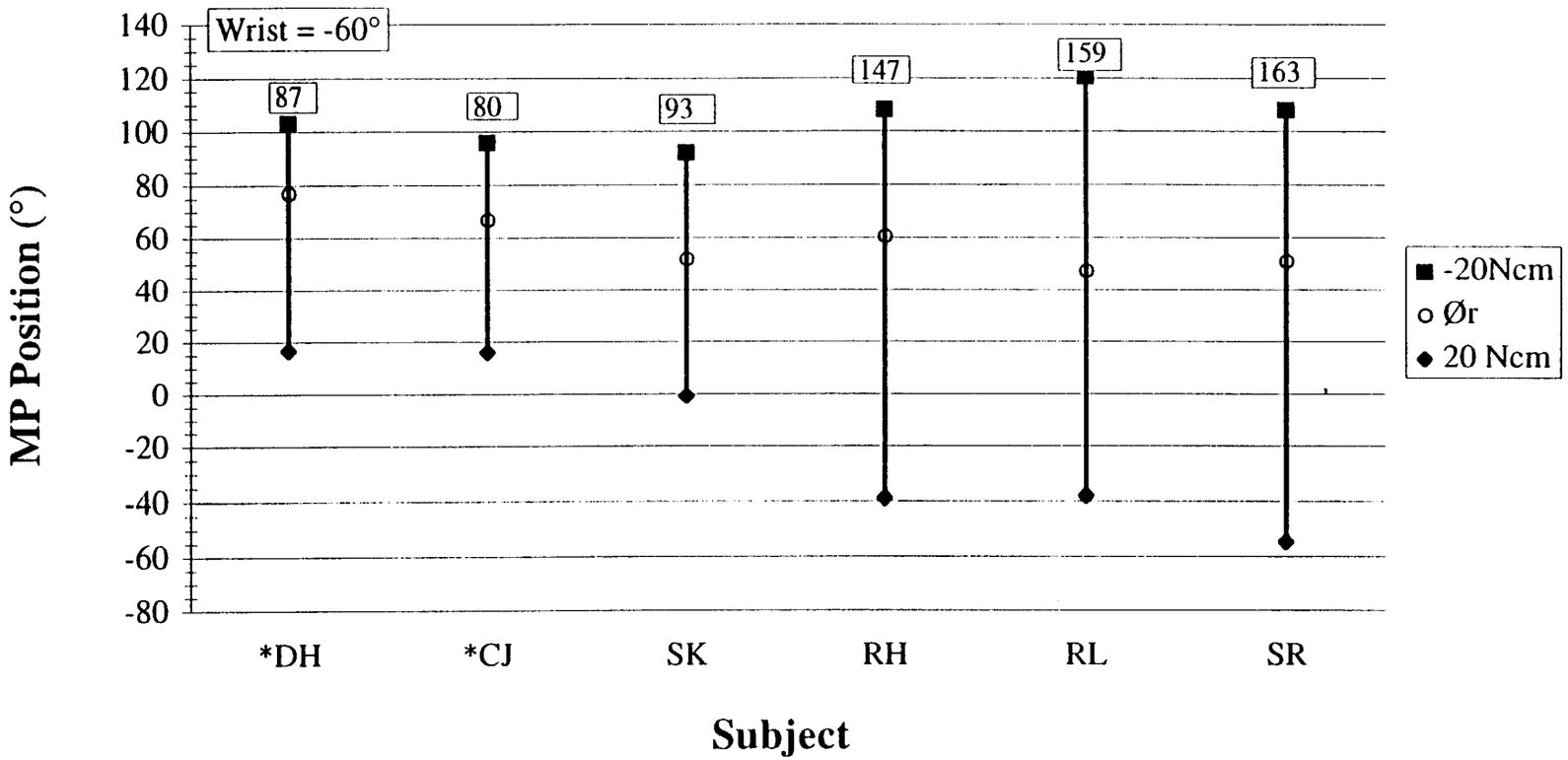

Figure 1.a.ii.16. PROM and Ør computed for each subject for the case when the wrist was fixed at 60° of extension. Subjects with an asterisk beside their initials are tetraplegic. The boxed values are the MP PROM between -20 and 20 N·cm.

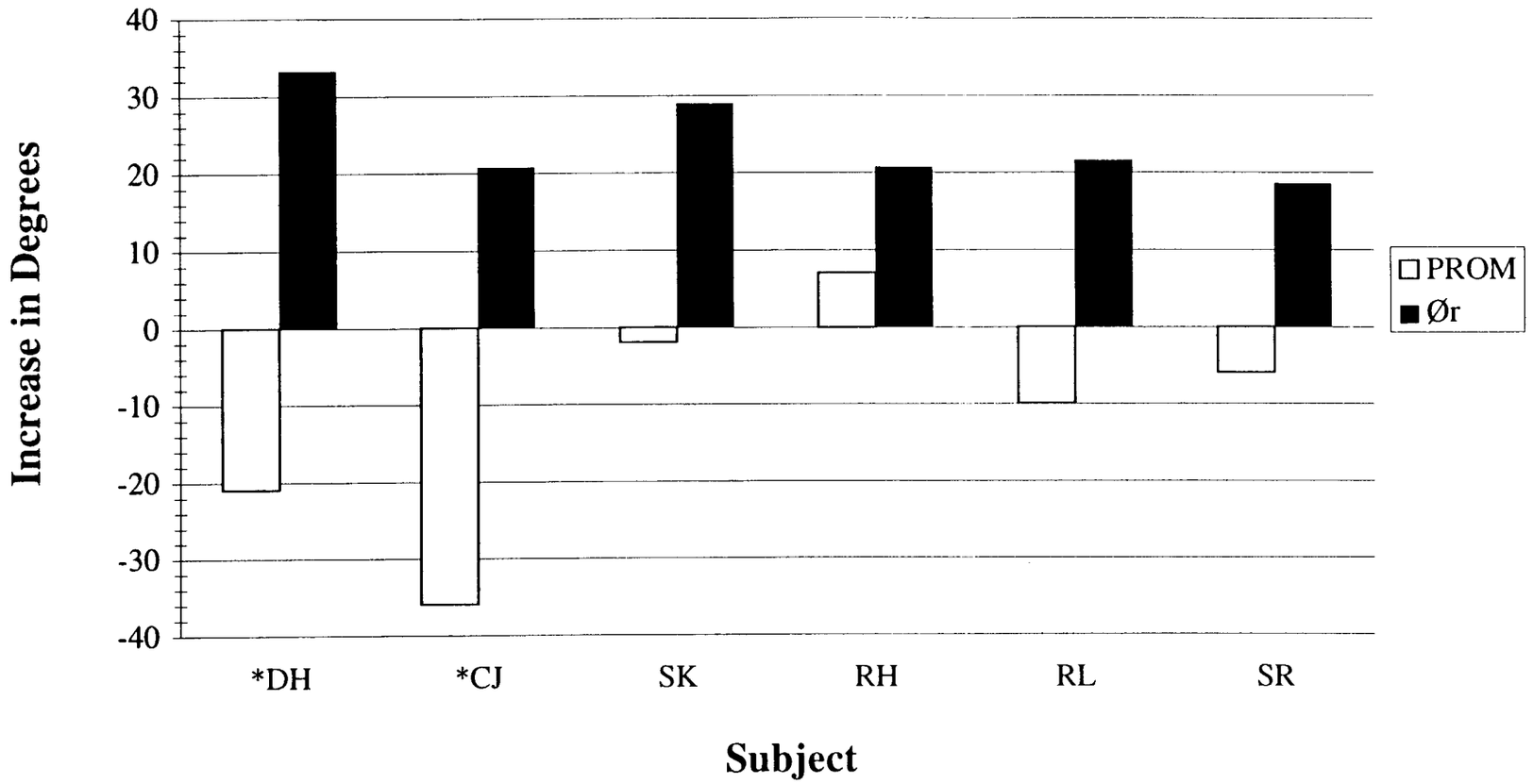

Figure 1.a.ii.17. The change in PROM and Ør for each subject as the wrist extends from 0° to 60°. Subjects with an asterisk beside their initials are tetraplegic.

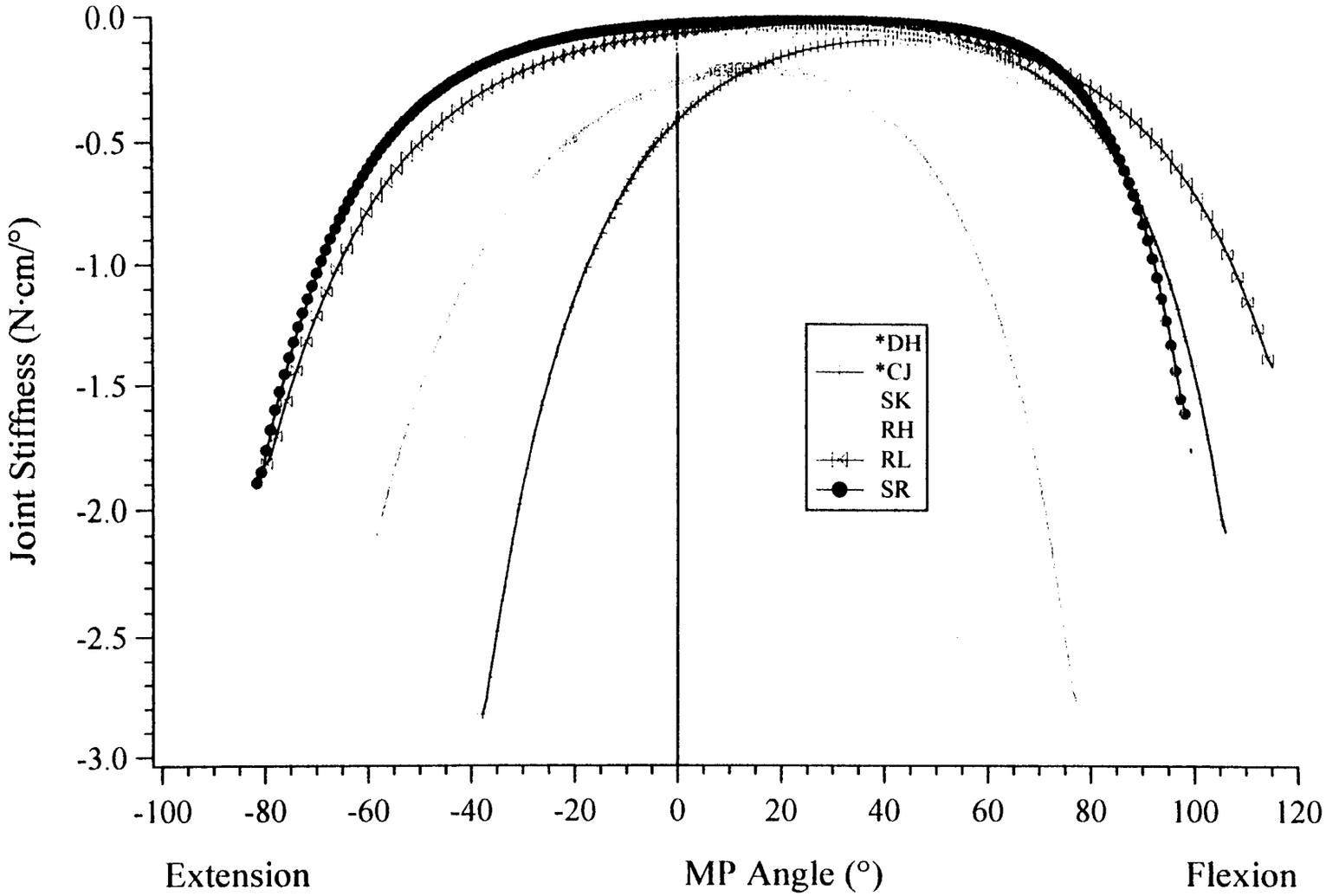

Figure 1.a.ii.18. Derivative of the curve fit for each subject for the case when the wrist was fixed at 0°. Subjects with an asterisk beside their initials are tetraplegic.

1. b. BIOMECHANICAL MODELING: ANALYSIS AND IMPROVEMENT OF GRASP OUTPUT

Abstract

This project does not start until year three of the project, as described in the proposal. However, two important tools are being developed in order to make the necessary biomechanical measurements with individual patients. First, the use of magnetic resonance images to determine joint moment arms is described in Section 1.a.i. Secondly, the measurement of passive moments across all joints of the hand is described in Section 1.a.ii.. When these tools are complete, we will begin making measurements on both normal and paralyzed patients.

Objective

The purpose of this project is to use the biomechanical model and the parameters measured for individual neuroprosthesis users to analyze and refine their neuroprosthetic grasp patterns.

2. CONTROL OF UPPER EXTREMITY FUNCTION

Our goal in the five projects in this section is to either assess the utility of or test the feasibility of enhancements to the control strategies and algorithms used presently in the CWRU hand neuroprosthesis. Specifically, we will: (1) determine whether a portable system providing sensory feedback and closed-loop control, albeit with awkward sensors, is viable and beneficial outside of the laboratory, (2) determine whether sensory feedback of grasp force or finger span benefits performance in the presence of natural visual cues, (of particular interest will be the ability of subjects to control their grasp output in the presence of trial-to-trial variations normally associated with grasping objects, and in the presence of longer-term variations such as fatigue), (3) demonstrate the viability and utility of improved command-control algorithms designed to take advantage of forthcoming availability of afferent, cortical or electromyographic signals, (4) demonstrate the feasibility of bimanual neuroprostheses, and (5) integrate the control of wrist position with hand grasp.

2. a. HOME EVALUATION OF CLOSED-LOOP CONTROL AND SENSORY FEEDBACK

Abstract

The purpose of this project is to deploy an existing portable hand grasp neuroprosthesis capable of providing closed-loop control and sensory feedback outside of the laboratory. Effort this quarter was devoted to preliminary laboratory testing of the portable feedback system and the evaluation task with four hand neuroprosthesis users. The compliant object was modified, reducing its weight by 87%, and was glued to the thumb-mounted sensor to obviate the need for subjects to manipulate (rather than simply squeeze) the object. Some of the subjects completed the task with or without vision, but others had difficulty. The preliminary results suggest that sensory feedback of grasp force can assist users in acquiring and maintaining a fixed grasp force.

Purpose

The purpose of this project is to deploy an existing portable hand grasp neuroprosthesis capable of providing closed-loop control and sensory feedback outside of the laboratory. The device is an augmented version of the CWRU hand neuroprosthesis, and was developed and fabricated in the previous contract period. The device utilizes joint angle and force sensors mounted on a glove to provide sensory information, and requires daily support from a field engineer to don and tune. The portable feedback system is not intended as a long term clinical device. Our goal, rather, is to evaluate whether the additional functions provided by this system benefit hand grasp outside of the laboratory, albeit with poor cosmesis and high demands for field support.

Report of Progress

Effort this quarter was devoted to preliminary laboratory testing of the portable feedback system and the evaluation task with four hand neuroprosthesis users. All subjects used a new object that was constructed for the evaluation task. The basic configuration of the new object is unchanged, but the material was changed from a foam and carbon fiber laminate to balsa wood; and the size was reduced slightly (new width = 3 cm). The change in material greatly reduced the weight of the object (from 116 gr to 14.8 gr) without compromising object rigidity. The weight reduction was especially important since the old object would often slip from the subject's grip unless a sticky surface (Dycem) was added to the object.

Subject 1:

This subject was tested with open-loop lateral grasp, with force sensory feedback delivered through an electrode mounted on the frontal aspect of the upper arm at the level of the axilla. The subject wore the modified FSR mounted on a guitar thumb-pick (as described in the preceding report). The threshold and comfort levels of the sensory feedback were set according to the protocol described previously, although the sensor calibration was not optimal (*see below*). Nonetheless, the subject reported feeling a graded output with variations in the command level.

The subject had difficulty picking up the object and only completed it successfully once by standing the object vertically and sliding her hand down over it. Because of restricted hand opening and hand postures, the subject could not pick the object up before pushing it away. Also, this subject had difficulty generating intermediate forces. Rather, the grasp force jumped from minimum to maximum and back, even though the subject could watch a force trace displayed on the computer monitor. Two representative force traces are shown in Fig. 2.a.1. The subject reported that she did not try to use intermediate forces for ADL and squeezed everything (utensil, pens, etc.) as firmly as possible. The all-or-nothing operation of the neuroprosthesis was a consequence of the subject's steep recruitment curves, verified by previous input-output testing. As a consequence, this subject is not a promising initial candidate for the portable sensory feedback system, but might benefit from closed loop control.

The difficulties this subject had in grasping the object lead to a redesign of the grasping task. It was clear that the performance would be compromised by poor control over object acquisition, independent of how well the subject could control their grasp. Sensory feedback and closed loop control would not be expected to assist significantly in acquisition, reducing the sensitivity and efficiency of the assessment task. As a result, the thumb-mounted force sensor was glued directly to the object, effectively instrumenting the object. The "instrumented object" could then be mounted and worn on the thumb via the clip, obviating the need to acquire the object. Note that this modification was made possible by the reduced weight of the new object described above. The "acquire" phase of the modified task will consist solely of squeezing the object to generate the required target force.

Subject 2:

Subject 2 had no trouble completing the task using the modified object mounted on the thumb. The subject could generate intermediate forces, and was able to complete several trials with a target command level of 60 ± 8% (without vision). The portable system was configured differently for this subject and used an alternative interface to the computer which proved problematic and prevented systematic data collection.

This subject is currently testing the bilateral hand-grasp system prototype and is not available for field tests of the PCLS.

Subject 3:

Subject 3 was very successful performing the evaluation task using lateral pinch with the left hand and the thumb-mounted instrumented object. The electrode was placed at the base of the subject's neck. The subject reported using the sensory feedback to reach and maintain the target force without prompting to do

so, and was able to complete the task with a variety of acquire and hold times and target window sizes and locations. Although time limited the number of trials that could be completed, it was clear that modification of the time intervals or the target windows would result in graded success rates. Representative force traces are shown in Fig. 2.a.2 for 60 ± 15% (top) and 40 ± 15% windows (bottom). Dashed traces represent trials performed with vision (i.e., the subject was allowed to watch the force trace), and solid lines are trials without vision.

The lengthy session with this subject identified several small bugs in the PCLS software that will be corrected in the next quarter.

This subject is an ideal candidate for PCLS testing, but does not live in the Cleveland area.

Subject 4:

This subject performed the task under the same conditions as subjects 2 and 3, using lateral grasp with the right hand. Again, the electrode was placed at the base of the neck. The subject was able to complete the task with difficulty, and reported weak and equivocal feedback stimulation. The stimulus settings were likely in error due to calibration problems (*see below*).

This patient has poor hand posture and grasp control, and is not an ideal candidate for field trials.

Calibration:

The new force sensor requires a logarithmic (see previous report) rather than a quadratic calibration. The PCLS software will be modified to accommodate a look-up table for calibration since the microcontrollers do not support floating point calculations readily. A larger problem that will be remedied is the use of fixed minimum and maximum forces in the stimulus-to-force mapping. The current software assumes that the minimum force is 2N and the maximum is 20N, regardless of the subject's actual grasp force. As a result, a weak subject will receive minimal stimulation even at 100% command. The force extrema will now be either set by the experimenter or linked to the measured force maximum of the individual subject.

Plans for Next Quarter

The PCLS software will be modified to correct the minor bugs discovered during lab testing, and to correct the important changes in the calibration protocol. Laboratory testing will be continued to determine if window size and acquire/hold times can be varied to yield graded performance. Again, we will canvas users to identify a willing candidate for field trials.

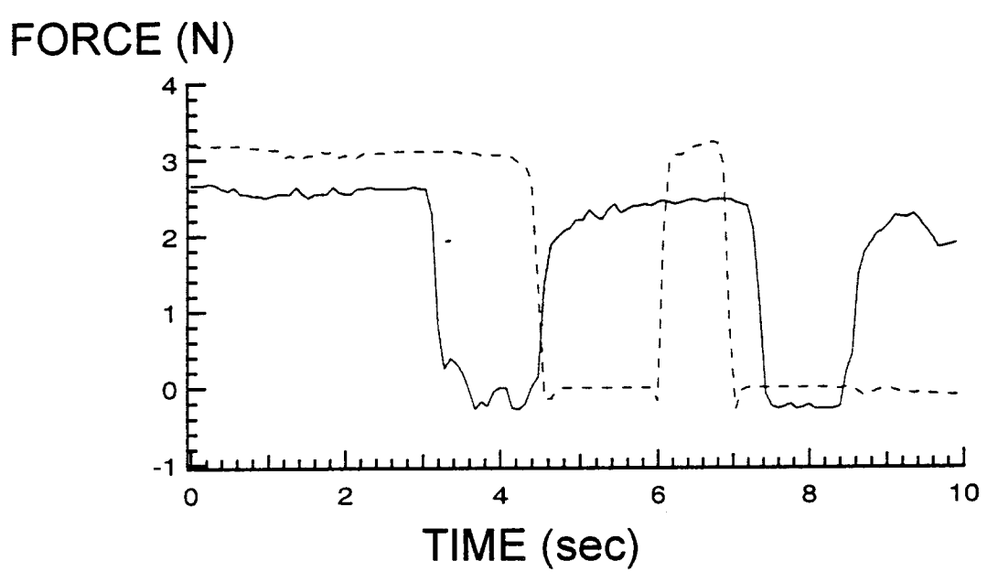

Figure 2. a. (1) Two force traces from subject 1. Forces are only approximate. The acquire and hold phases were both 5 seconds. The subject was unable to produce intermediate forces because of steep recruitment curves.

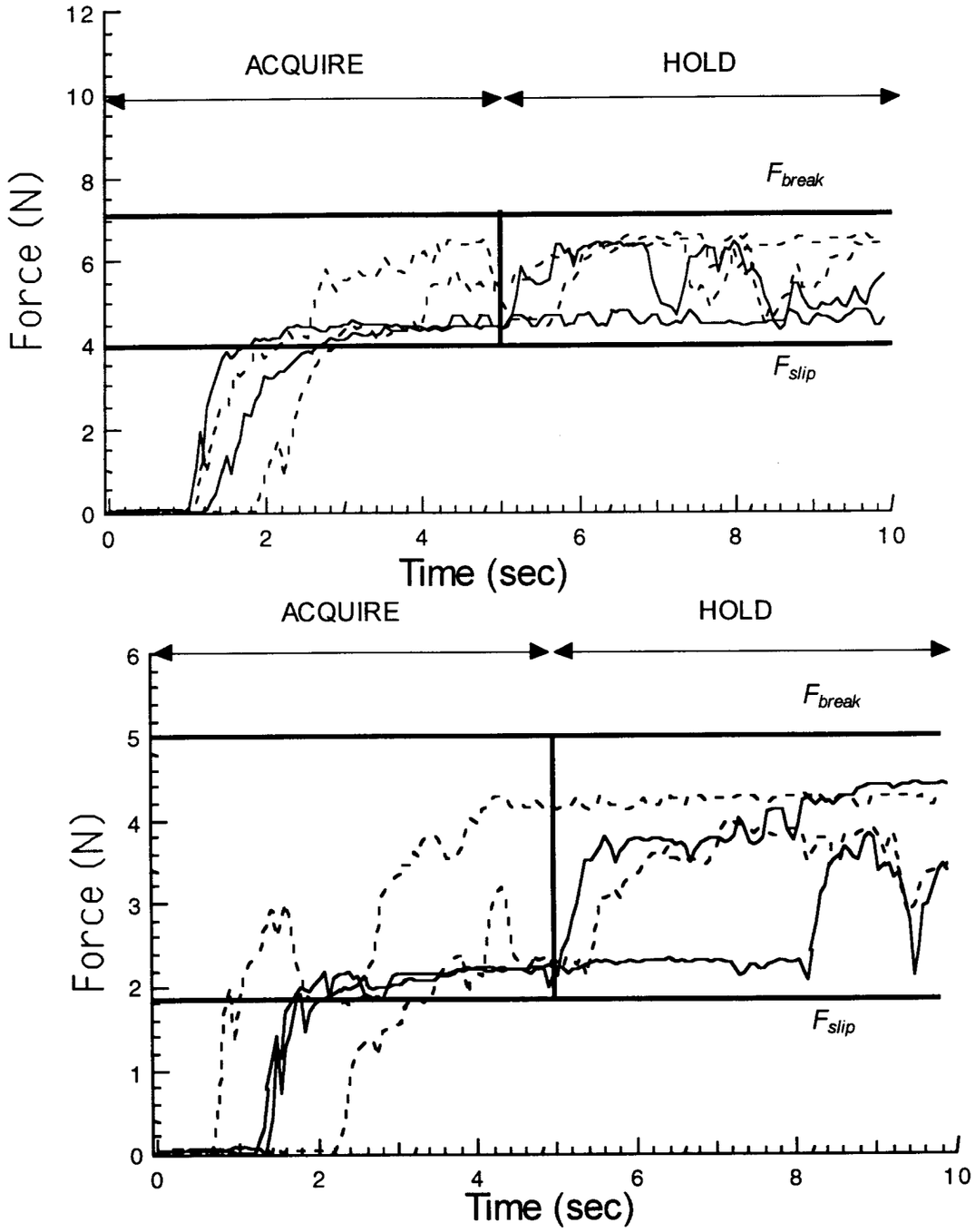

Figure 2. a. (2) Two sets of trials for Subject 3. Target windows (in command level) were 60 ± 15% (top) and 40 ± 15% windows (bottom). Dashed traces represent trials performed with vision (i.e., the subject was allowed to watch the force trace).

2. b. INNOVATIVE METHODS OF CONTROL AND SENSORY FEEDBACK

2. b. i. ASSESSMENT OF SENSORY FEEDBACK IN THE PRESENCE OF VISION

Abstract
The purpose of this project is to develop a method for including realistic visual information while presenting other feedback information simultaneously, and to assess the impact of feedback on grasp performance in the presence of such visual information. All components of the video simulation system have been developed and tested. The components will be integrated onto a new computer platform in the next quarter.

Purpose

The purpose of this project is to develop a method for including realistic visual information while presenting other feedback information simultaneously, and to assess the impact of feedback on grasp performance. Vision may supply enough sensory information to obviate the need for supplemental proprioceptive information via electrocutaneous stimulation. Therefore, it is essential to quantify the relative contributions of both sources of information.

Report of Progress

All of the video capture hardware (Video Vision PCI video capture board) and software (Radius Edit) has bee acquired, and functional prototypes of all of the major components of the video system have been developed and tested. As described previously, video clips will be recorded of a neuroprosthesis user's hand squeezing an object while the command signal is ramped over its full range under computer control. Force and span signals will be recorded at the same time. Each video frame will be associated with a particular command level, a grasp force, and a finger span. At a later time, and able-bodied subject will be able to don a shoulder controller, exert a particular command level, and thereby recall the appropriate video frame, force and span. The video will simulate realistically actual motor control of a neuroprosthesis, and the force and span data will be used to synthesize appropriate sensory feedback.

The most important component of the system is the program for retrieving frames from a video clip upon demand. That program has been written and can play back a video clip frame-by-frame, in arbitrary order, at 30 frames per second, in 16-bit color, and with 640x480-pixel frames. The quality of that video is not noticeably different than the same clip played in the normal frame sequence.

A method has also been developed to synchronize and process the video, force, and span data. Briefly, a computer signal is used to initiate both video recording and data sampling, the former at 30 frames per second and the latter at 300 samples per second. A beeper is triggered manually after a brief delay, and the sound signal is captured on the audio track of the video tape and an analog sampling channel. The audio track is subsequently analyzed with a video editing program to identify the starting video frame. The sampled audio signal is analyzed with a threshold detector to determine the starting sample. Starting with the first complete video frame (the audio signal will, in general, begin part way through a frame), the command, force, and span data are averaged, taking the middle 8 points of the 10 collected during the frame. A correction is periodically applied since the sampling rate (300 Hz) is not an exact multiple of the frame rate (29.97 frames/second). The result of the processing is an array where each row corresponds to a particular frame number and contains an average command, force and span associated with that frame.

The data collection method has been implemented and tested with one of the neuroprosthesis users to create example data files for assembling and testing the complete video simulation system. All of the components were tested on a Power Computing Power Wave 604 (dedicated to a different project). A Power Computing PowerTower 225 has been acquired for this project, and the different components are being transferred to and integrated on the new platform.

Plans for Next Quarter

The complete simulation system will be completed and tested on the new computer.

C. 2. b. ii. INNOVATIVE METHODS OF COMMAND CONTROL

Abstract

During this quarter we completed development of hardware and software for evaluation of nail mounted strain gages for object contact detection during grasp. We also fabricated a set of six standard objects to use during these evaluations. The strain gage sensor was tested on four subjects with three completing the standard protocol. The results of these studies demonstrate that a nail mounted strain gage provides greater than 90% detection of contact for most objects, with an overall contact detection rate of 85%. This detection rate was accompanied by a large number of false positives, primarily the detection of object release.

Purpose

The purpose of this project is to improve the function of the upper extremity hand grasp neuroprosthesis by improving user command control. We are specifically interested in designing algorithms that can take advantage of promising developments in (and forthcoming availability of) alternative command signal sources such as EMG, and afferent and cortical recordings. The specific objectives are to identify and evaluate alternative sources of logical command control signals, to develop new hand grasp command control algorithms, to evaluate the performance of new command control sources and algorithms with a computer-based video simulator, and to evaluate neuroprosthesis user performance with the most promising hand grasp controllers and command control sources.

The first objective is to identify and evaluate alternative sources of logical command control signals. We will investigate object contact and object slip detection using sensors mounted on the dorsal surface of the thumb. The first sensor investigated was a strain gage glued to the thumbnail and used to detect object contact.

Report of Progress

During this quarter we completed hardware and software development to evaluate contact sensor outputs during grasp. We have fabricated a set of six standard objects and completed evaluation of the sensor in three subjects.

METHODS

All subjects read and signed an informed consent, and all procedures were reviewed by the Institutional Review Board of MetroHealth Medical Center.

A metal foil strain gage (SG-3/350-LY13, Omega Engineering, Stamford, CT)) was glued to the thumbnail of the dominant hand approximately perpendicular to the long axis of the thumb, using cyanoacrylate cement (fig. C.2.b.ii.1A). A custom-built instrumentation amplifier, based around the Analog Devices 1B31AN chip, was used to provide excitation voltage (5V), amplification, and low-pass filtering (25 Hz) of the strain gage signals. The subjects were also instrumented with a large carbon rubber surface electrode (6282, 3M Health Care, St. Paul, MN) that formed 1 pole of a continuity detector. The other pole of the continuity detector was formed by conductive foil placed on one side of each of the test objects (fig. C.2.b.ii.1A). A custom-built detector generated a 5V signal when the hand-object circuit was completed and was used to provide an independent measure of when the thumb contacted the object to be grasped. Objects were placed on a table switch that generated a 5V signal when the object was lifted off the table.

Table C.2.b.ii.1: Physical Characteristics of the Test Objects

OBJECT	Diameter/Thickness (cm)	Mass (g)
Cylinder1	1.8	[illegible]
Cylinder2	4.2	[illegible]
Cylinder3	6.4	[illegible]
Block1	1.2	[illegible]
Block2	2.3	[illegible]
Block3	3.5	[illegible]

Six different objects were tested with each subject including three cylinders grasped with palmar grasp, and three blocks, grasped with lateral grasp. Each object was fabricated from [illegible] and all were covered on one surface with conductive foil. The objects sizes and weights are given in Table C.2.b.ii.1.

Each trial consisted of the subject reaching out, grasping, lifting, holding, replacing and releasing the object, and then returning their hands to the relaxed position. The beginning of a trial was preceded by an audio tone which signaled the subject to be ready. Approximately 1 s. after the tone an LED "GO" light came on to trigger the subject to begin the task. After the subject had grasped and lifted the object an LED "HOLD" light came on, triggered by the table switch. The "HOLD" light remained on for a pre-determined interval (2-3 s.) during which time the subject held the object. After the HOLD light turned off, the subject returned the object to the table, released it, and relaxed. Each subject conducted 10 trials with each object. On random trials, subjects were instructed to grasp but not lift the object or to position their hand but not contact or lift the object.

RESULTS

The output of the strain gage was affected by the position of the thumb, as well as contact of the thumb with the object to be grasped. Figure C.2.b.ii.1B shows the output of the gage for the complete task of reach, grasp, lift, hold, replace, release, and relax (*left*), for a trial where the object was grasped but not lifted (*center*), and for a trial where the hand was positioned, but the object was not lifted (*right*). During the complete task, the strain gage exhibited a triphasic output. The initial positive going phase of the strain gage signal corresponded to extension of the thumb to get around the object. The subsequent negative going phase corresponded to force application to the object by the thumb. Note that as compared to when the object was lifted (*left*), grasp only (*center*) produced a smaller force transmitted to the thumbnail (i.e., a smaller amplitude of the second phase of the signal). The third positive going phase corresponded to release of the object, and finally the signal returned to baseline as the thumb was relaxed. As seen in the right column, positioning alone also produced changes in the strain measured in the thumbnail, as a result of changes in the thumb position.

We found that the peaks of the high pass filtered strain signal corresponded well to when the object was contacted, and that a simple thresholding of the high pass filtered signal could be used to detect contact. All strain gage signals were high pass filtered at 0.5 Hz with a bi-directional second-order Butterworth filter. The bi-directional filter yielded fourth order magnitude filtering with perfect preservation of phase information. Amplitude thresholds to detect contact in the filtered signals were selected by eye, and thus are not optimized to minimize detection of either false positive or false negatives. In general, the high pass filtered signal gave a robust spike when the object was contacted (fig. C.2.b.ii.1B). When the object was contacted, but not lifted, a large spike was still present in the filtered strain signal. Note that in this example, the sensor was equally good at detecting object release. That is, there was an equally large spike in the filtered strain signal during object release. This feature led to a large number of false positives (see below), but can be eliminated by adding hysteresis to the detection algorithm. In this example hand positioning alone did not generate a suprathreshold level in the high pass filtered signal, however, in general there were false positives detected by thresholding the high pass filtered signal.

To determine the reliability of contact detection we had individuals repeatedly grasp, lift, and release the 6 standardized objects using either palmar or lateral grasp. Figure C.2.b.ii.2 shows the results of 162 trials across 3 subjects, not including random trials of grasp only or hand positioning without grasp. Figure C.2.b.ii.2A shows the number of contacts that were detected successfully, expressed as a

percentage of the number of trials. Each bar within a group represents one of the subjects, and the different groups of bars are the six different objects, listed across the bottom of the figure. In this analysis the threshold level for contact detection was the same across all objects for a given subject, but did vary between subjects. Overall, 85% of the contacts were detected correctly, however, in most cases the success rate was greater than 90%.

Figure C.2.b.ii.2B shows the number of false positives detected, again expressed as a percentage of the number of trials. In some cases the measure is greater than 100% because more than one false positive could be detected in a given trial. The false positives are further segregated to illustrate that the large majority of them occurred as a result of detection of object release, as was shown in the earlier example (fig. C.2.b.ii.1B). Other false positives were associated with changes in grasp force while the object was being held and changes in thumb position either before the object was grasped or after the object was released.

These data demonstrate that the thumbnail mounted sensor provided reliable detection of object contact across a variety of object sizes and across different grasps. However, the sensor also provided false detection of object contact, primarily during object release.

Plans for Next Quarter

During the next quarter we will investigate the use of "Receiver Operator Characteristics" and different filtering options to optimize contact detection. We will also record the output of the sensor when mounted on the instrumented hand of neural prosthesis users while they grasp and manipulate various objects.

In these experiments there was co-variation of object size and weight (Table C.2.b.ii.1), and thus these data do not allow us to determine the effects of these factors in contact detection. It appears that the lightest, smallest objects gave the poorest results (fig. C.2.b.ii.2A). In the next quarter we will continue testing using different weights of the standardized objects to isolate the effects of object size and object weight on contact detection.

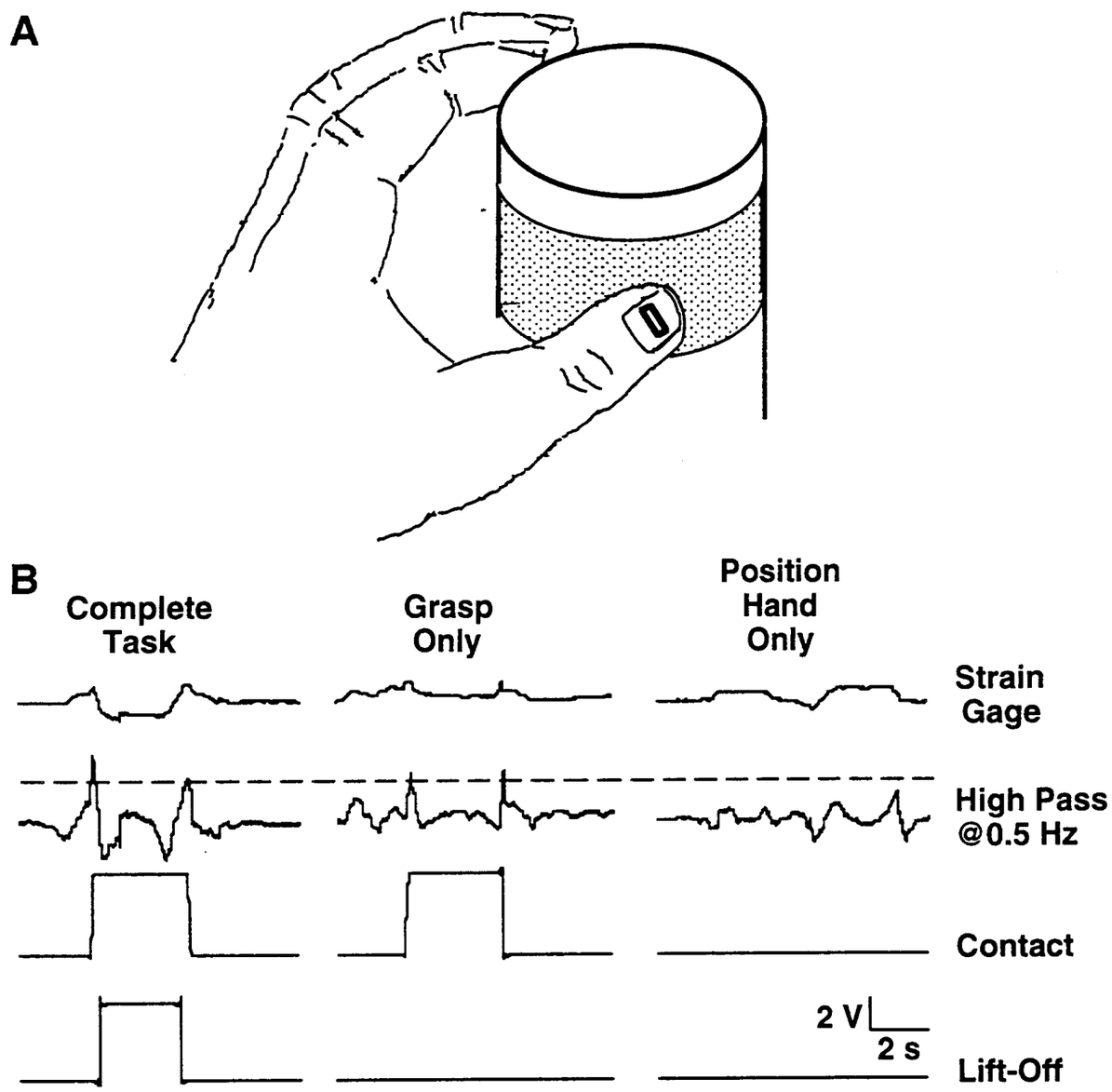

Figure C.2.b.ii.1: A thumbnail mounted strain gage was investigated as a contact sensor. A.) A foil strain gage was glued to the thumbnail with cyanoacrylate cement and the output of the gage was monitored while the subject grasped, lifted, replaced, and released a variety of objects. The objects were also instrumented with a conductive foil (*shaded*) to provide an independent signal indicating when the thumb contacted the object. B.) In addition to trials of object grasp, lift, replace, and release as shown in the left column, random trials where the object was grasped, but not lifted, as shown in the central column, as well as trials where the hand was positioned around the object, but the object was not grasped, as shown in the right column, were also included.

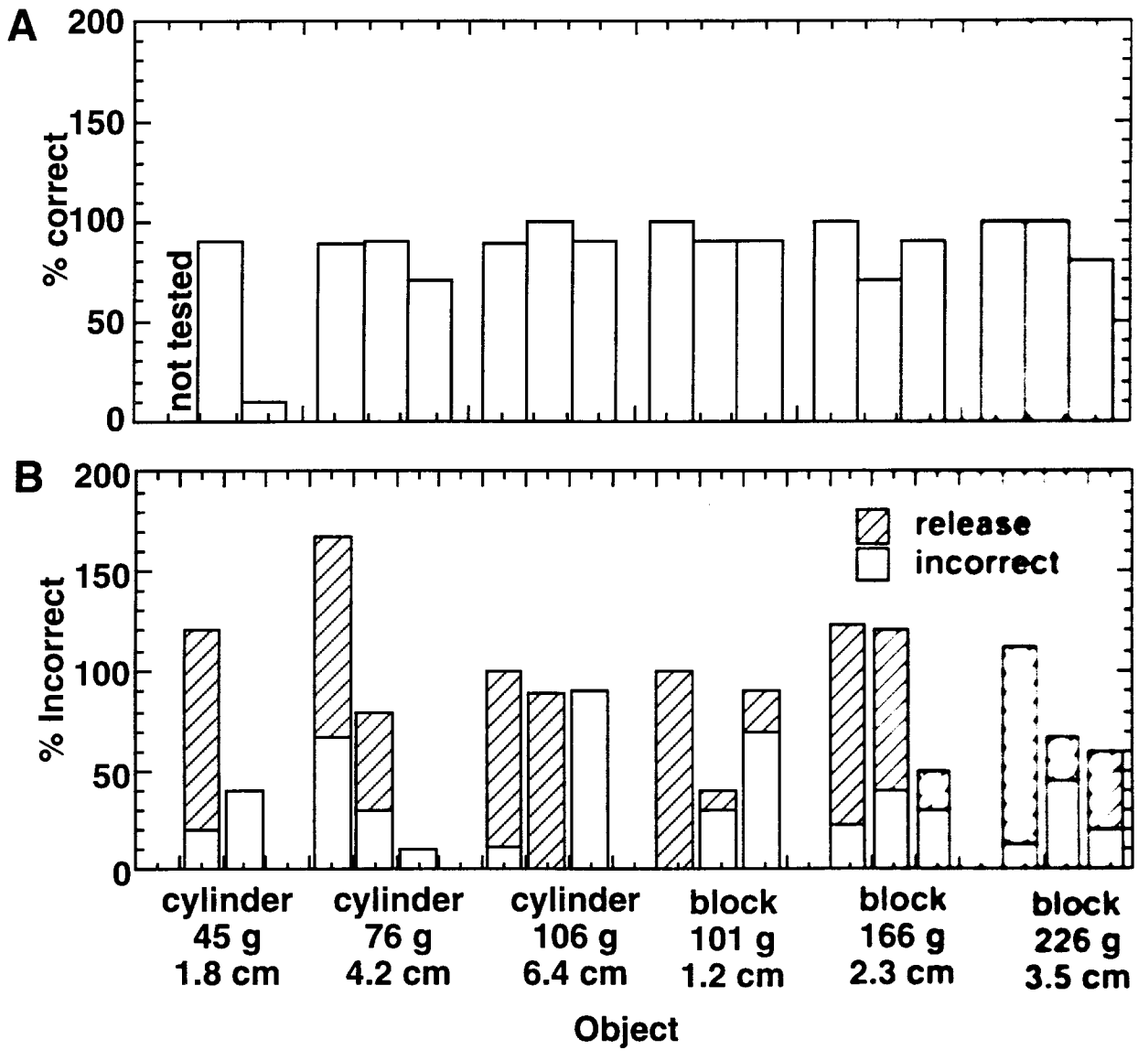

Figure C.2.b.ii.2: Results from three subjects using a thumbnail mounted strain gage to detect object contact. Each bar within a group is the result of one subject, and the different groups of bars are the results with different objects. A.) Number of correct contact detections, expressed as a percentage of the number of trials. The mean detection rate was 85%, but detection was 90% or better for most objects. B.) Number of incorrect detections (i.e., false positives), expressed as a percentage of the number of trials. Because more than one false positive could be detected in a given trial, this measure may exceed 100%. Further classification of incorrect detections indicated that most of the incorrect detections were associated with object release.

2. b. iii. INCREASING WORKSPACE AND REPERTOIRE WITH BIMANUAL HAND GRASP

Abstract
Bimanual control of hand grasp was implemented in one person, who already had an implanted hand grasp neuroprosthesis in the contralateral upper extremity. The added function provides palmar grasp using percutaneous intramuscular electrodes. Two switches are used for command/control. The individual is using the system on a take-home basis.

Purpose
The objective of this study is to extend the functional capabilities of the person who has sustained spinal cord injury and has tetraplegia at the C5 and C6 level by providing the ability to grasp and release with both hands. As an important functional complement, we will also provide improved finger extension in one or both hands by implantation and stimulation of the intrinsic finger muscles. Bimanual grasp is expected to provide these individuals with the ability to perform over a greater working volume, to perform more tasks more efficiently than they can with a single neuroprothesis, and to perform tasks they cannot do at all unimanually.

Report of progress
In this quarter, preliminary research was done in preparation for a more intensive study of the problems associated with bimanual control. This included the implementation of bimanual control in one of the current neuroprothesis users to test the feasibility of its use by a human subject and to identify deficiencies. The subject was provided the system for home use so that he could report his experience in daily task performance. This has enabled us to identify issues concerning the control of a bimanual system and the means to evaluate bimanual performance with activities of daily living (ADL) tasks.

The subject that was selected for this study was a current neuroprothesis user (JHJ) who has an implantable 8 channel stimulator in his left hand. He has C6 function in his left arm and C5 in his right. The subject uses wrist position for command control and a manual switch for grasp selection/hold. The neuroprothesis provides him with both palmar and lateral prehension on that side. On the subject's right side, a percutaneous system was implemented. The subject was only provided with palmar prehension in his right arm because of adductor pollicis (AdP) denervation. A wrist hand orthotic was also used since there is no activate wrist extension on that side.

A primary focus of the implementation was the command control signal for JHJ's right hand. The lack of active wrist extension in JHJ's right arm negated the use of wrist position for command control. Also, contralateral shoulder control could not be used since it would interfere with the operation of the implanted system on the left side. Therefore, an additional means of controlling the system to allow for home usage had to be found. An attempt was made to use the brachioradialis (BR) muscle as a source for the control signal. Using a clinical system which has been developed to use EMG as a control source, percutaneous electrodes were inserted into the BR and the signal was used to control hand opening and closing. However, the EMG signal proved to be too noisy even after filtering and signal processing. It was concluded that the noise was due to the fact that a percutaneous system was being used on that side. The return anode on the surface of the skin in the area of the biceps brachii forces the return current through the BR muscle in part, and this was being picked up by the electrodes in the muscle. These are problems that can be resolved, but for expediency were not pursued at the current time.

An alternative for controlling the right hand was to use switch control. Since the subject has only one type of grasp in the right hand, a simple system of two switches was implemented. One switch controlled the power to the system while the second switch gated the command which controlled hand opening and closing (Peckham, et al. 1980). The gated ramp had a 0.75 sec delay with a two second ramp between full open to full hand closure. This solution has allowed the subject to begin the use of bimanual control at home, but it is only a temporary solution. Clearly the issue of command control has to be investigated more thoroughly.

The implementation of the switch control on the right hand side allowed for some evaluation of bimanual control to be made. The subject was first trained using the bimanual system for eating with both hands. For the eating tasks, the subject did not show greater proficiency with the use of both hands since he was very skilled with one handed eating. However, one observation that was made was that the subject's workspace did increase. With one handed eating, the subject had to switch grasps to go from eating with a fork to drinking, and all objects had to be moved directly in front of him to be grasped. With the bimanual system, the subject was able to keep the fork in one hand and use the other to drink or grasp another object. Also, the subject did not have to manipulate objects in the workspace as much in order to acquire them. Full task evaluation has not been performed.

Plans for Next Quarter

During the next quarter, more focus will be placed on addressing the control issues that a bimanual system presents. More effort will be placed into implementation of EMG for command control as well as research into other possible control schemes. Also, more effort will be placed on evaluation of the bimanual system with ADL tasks. This will include more training with the current subject on two handed tasks. Finally, effort will be placed on the evaluation of the intrinsic muscles in the hand grasp to improved finger extension. This will included measurements of joint angle, contact and grip force with and without the intrinsic muscles, and joint moment curves as measured with the finger moment transducer.

References

Peckham PH, Marsolais EB, Mortimer JT. Restoration of key grip and release in the C6 tetraplegic patient through functional electrical stimulation. Journal of Hand Surgery. 1980; 5(5): 462-469.

2. b. iv CONTROL OF HAND AND WRIST

Abstract

Wrist extension moments must be capable of balancing the flexion moments in order to establish an equilibrium in a functional position. Feedforward methods may be capable of establishing equilibrium since many of the muscles are under stimulation control, and thus many of the sources of wrist moments are known to some extent. We show in simulation studies of lateral grasp that feedforward control can be established with artificial neural networks, allowing isolated control of wrist angle and hand grasp.

Purpose

The goal of this project is to design control systems to restore independent voluntary control of wrist position and grasp force in C5 and weak C6 tetraplegic individuals. The proposed method of wrist command control is a model of how control might be achieved at other joints in the upper extremity as well. A weak but voluntarily controlled muscle (a wrist extensor in this case) will provide a command signal to control a stimulated paralyzed synergist, thus effectively amplifying the joint torque generated by the voluntarily controlled muscle. We will design control systems to compensate for interactions between wrist and hand control. These are important control issues for restoring proximal function, where there are interactions between stimulated and voluntarily controlled muscles, and multiple joints must be controlled with multijoint muscles.

Report of progress

The goal of the wrist control project is to provide active and appropriately graded wrist extension moments to counteract the prominent wrist flexion moments generated by hand grasp muscles. If we can accomplish this, we will be able to eliminate the dorsal wrist support orthosis that C5 and weak C6 patients must weart, and they will be able to go brace free. We will also be able to separately control the wrist angle to facilitate object manipulation.

We showed in the last Quarterly Progress Report that strength can be increasd sufficiently by tendon transfers. The current Progress Report will concentrate on our control studies.

Isolating hand grasp and wrist control is a challenging problem since most of the finger and thumb muscles also cross the wrist, producing significant wrist flexion during grasp (see Figure 2.b.iv.1). Similarly, changing wrist angle can alter grasp.

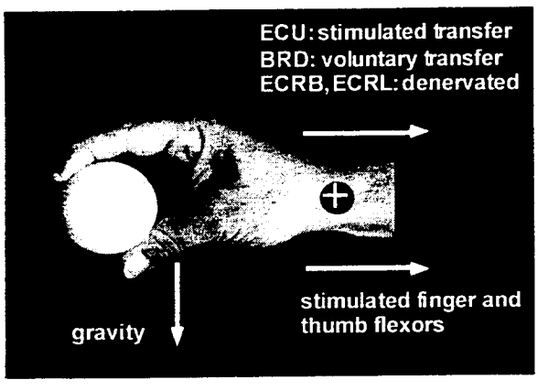

Figure 2.b.iv.1. Major contributors to wrist moments in individuals with C5 or weak C6 tetraplegia. The stimulated extrinsic finger and thumb flexors cause significant wrist flexion moments, as does gravity when the forearm is pronated. The sources of extension moments are limited. The strongest sources are normally the ECRB and ECRL, but they are almost always denervated in this population, and hence can not be stimulated. If the ECU is not denervated, then it can be transferred into the ECRB tendon and stimulated. If the BRD can be activated voluntarily, then it can also be transferred into the ECRB tendon to provide some voluntary control. Significant wrist moments also arise from the passive structures crossing the joint, but these are not shown.

However, since nearly all the muscles are under stimulation control, it may be possible to compensate for many of the interactions with a feedforward control system, rather than a feedback control system such as we demonstrated earlier [Lemay and Crago, submitted]. This would be a significant improvement, since it would eliminate the need for a feedback sensor.

We are investigating feedforward control first in simulation, using the dynamic model of the arm and hand that we developed previously [Estecki and Mansour 1996; Lemay and Crago 1996]. This report covers our work on lateral grasp.

Feedforward Controller Structure

The feedforward controller (see Figure 2.b.iv.2) consists of two stages, the first of which specifies the coordination of the hand and wrist in terms of grasp force, grasp opening, wrist angle, and finger angle commands. This *coordination network* is an extension of the grasp template Kilgore et al. [1993] has developed to synthesize hand grasp.

The second stage specifies the muscle activation levels to all of the involved muscles in terms of the grasp and wrist templates. We call these the *interaction networks* since they must account for the biomechanical interactions. The function of these networks is to encode the pulse width maps.

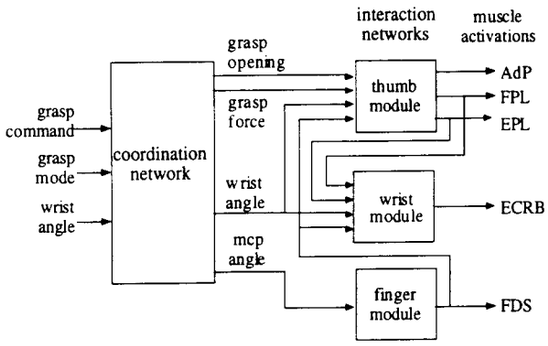

Figure 2.b.iv.2 Feedforward controller for isolating wrist and hand grasp. The coordination network converts the grasp and wrist commands into desired kinematic and force variables (grasp and wrist templates). The interaction networks convert the templates into the activations that will ideally produce the desired kinematic and force outputs. The interaction networks must take into account the interaction between wrist posture and hand grasp.

We used separate interaction network modules for the thumb, the wrist, and the finger. Each module was implemented with an artificial neural network (ANN) that was trained with input-output data from simulations.

For example, the wrist module specifies the activation level for the wrist extensor (ECRB), taking into account not only the desired wrist angle, but also the stimulation levels to the index finger and extrinsic thumb muscles (but not the intrinsic thumb muscle, adductor pollicus, since it produces no wrist moment).

Interaction Network Design and Training

The three interaction modules for lateral grasp (wrist, finger and thumb) were designed on the basis of the biomechanical interactions observed in simulation, and trained with input-output data obtained from simulations. The networks were tested with data that was not part of the training set (see the Performance section that follows). The design and taining results will be summarized separately for each module.

Wrist Module

The purpose of the wrist module is to specify the activation level of the wrist extensor (ECRB) required to achieve equilibrium at the desired wrist angle. The activations to the extrinsic hand muscles must be included as input to the wrist module since stimulation of the hand extrinsic muscles generates additional muscle moments about the wrist, thus affecting wrist position. For example, in Figure 2.b.iv.3, wrist angle was plotted against ECRB activation for different values of thumb flexor activation (FPL) and thumb extensor activation (EPL) (steady state data obtained with simulations using the dynamic model of the arm). To obtain a wrist angle of 0° with no FPL activation (but FDS activation equal to 0.1--see next paragraph), the ECRB activation must be 0.0568 (Figure 2.b.iv.3, left). However, when the FPL activation was increased to 0.30, an additional flexion moment at the wrist was generated. Therefore, the amount of ECRB activation needed to maintain a 0° wrist angle increased to 0.2963. Similarly, when the EPL was not activated, the ECRB activation needed to reach a 10° wrist extension was 0.0782 (Figure 2.b.iv.3, right). Once the EPL was activated to 0.3, the additional extension moment at the wrist resulted in a decrease in ECRB activation needed to maintain 10° wrist extension (ECRB activation equal to 0.0229). Therefore, the activation level of the extrinsic hand muscles were included as inputs to the wrist module.

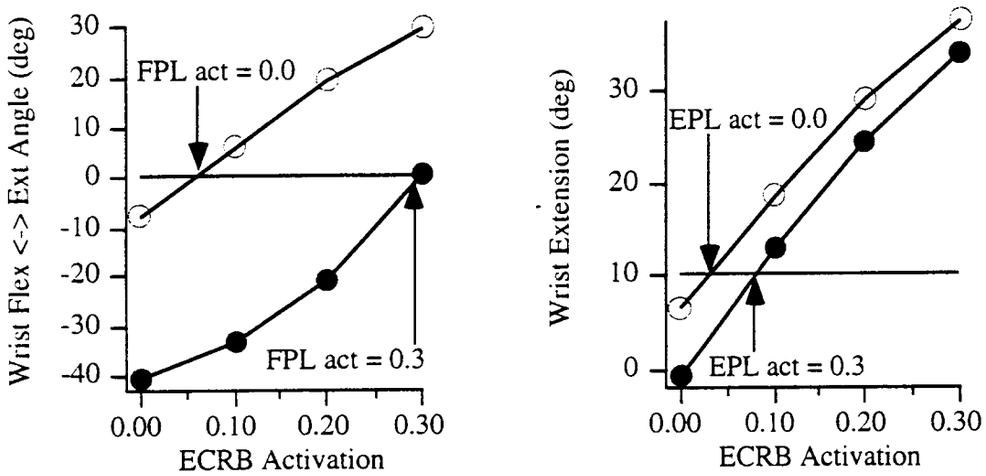

Figure 2.b.iv.3. Wrist Angle as a function of ECRB activation for different levels of FPL activation (left) and EPL activation (right). Note that for the laft hand graph, FDS activation was set at 0.10, while for the right hand graph, FDS was not activated.

The wrist module was implemented with a radial basis artificial neural network (as were the other interaction networks). Training data were obtained with a the dynamic model of the arm in two sequential phases. In the first phase, the ECRB activation level was stepped from 0 to 0.3 in increments of 0.1 for different FPL activation levels (0, 0.05, 0.1, 0.2, 0.3), and the steady state wrist flexion/extension angle was calculated. In addition, for each FPL activation level, the ECRB activation value where the resulting wrist angle was 0° was included in the training data. The FDS activation level was constant at 0.1 because in the lateral grasp templates, the fingers flexors are activated before the thumb flexors in order to form a base for the object. The EPL was not activated in these simulations (i.e. no co-contraction of thumb flexor and extensor).

In the second phase, the ECRB activation level was stepped from 0 to 0.3 in increments of 0.1 for different EPL activation levels (0, 0.1, 0.2, 0.3), and the resulting wrist flexion/extension angle was calculated. Also included in the training data was the ECRB activation value where the resulting wrist angle was 0° for each EPL activation level. These simulations were performed with FDS activated at 0.0 and 0.1, since the activation of the thumb extensors can overlap the activation of the finger flexors in lateral grasp templates. The FPL was not activated in these simulations.

The training of the wrist module (as well as the other interaction networks) was done in MATLAB with the Neural Network Toolbox with the data from both phases. The inputs to the network were wrist angle (normalized), FPL activation, FDS activation and EPL activation. The output was the corresponding ECRB activation. The radial basis neural network algorithm in MATLAB increases the number of hidden neurons automatically in order to reach the desired error goal. The end result of the training process was an artificial neural network with 19 hidden neurons and a sum square error of 0.0024 (dimensionless activation level squared).

Finger Module

The function of the finger module in lateral grasp is to specify the index finger activation required to maintain the desired index finger position during grasp. In this design, the finger position was represented as metacarpopalangeal (MCP) flexion angle. Only the desired MCP angle needed to be an input to the finger module since simulations showed that neither grasp force or wrist angle had a significant effect on MCP angle under these conditions (Figure IIIa and Figure IIIb).

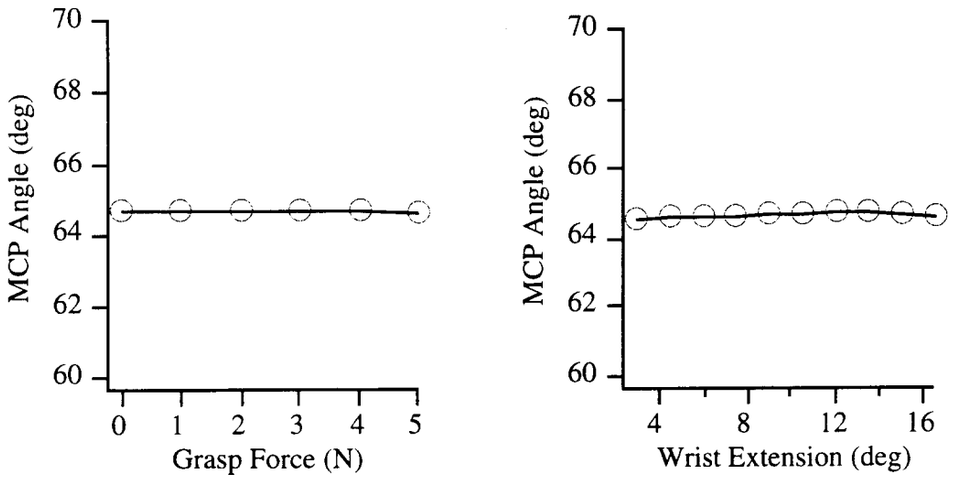

Figure 2.b.iv.4. MCP angle flexion as a function of grasp force (left) and wrist extension (right) when FDS activation was constant at 0.10

The finger module was also implemented as a radial basis neural network. To obtain the training data, simulations with the dynamic model of the arm were performed, where the FDS activation level was set at either 0, 0.05, or 0.1, and the MCP angle was calculated. The maximum activation level for the FDS was set at 0.1 since: (1) the resulting MCP angle was approximately 64° flexion, which is enough flexion to form a base for an object in lateral grasp, and (2) additional simulations revealed that strong FDS and FPL activation combined with weak ECRB activation can produce negative stiffness at the wrist, resulting in unstable wrist posture. This must be explored in further simulations, but should also be examined experimentally.

The training of the finger module was done in the same way as the wrist module. The MCP angle was the input and the FDS activation level was the output. Since the network had only one input, the number of hidden neurons needed to reach the desired error goal was only two (sum square error goal = 0.0001).

Thumb Module

The function of the thumb module is to control grasp opening and grasp force by specifying the activation of the thumb muscles. FDS activation and wrist angle were also included as inputs to the thumb module to account for interactions. In the model, the FDS acts as an ulnar deviator at the wrist, thus increasing grasp opening. In the opposite manner, wrist extension combined with radial deviation will decrease grasp opening. However, the combination of FDS activation and wrist extension can have different effects on grasp opening, as seen in Figure 2.b.iv.5 and Table 2.b.iv.1. In Figure 2.b.iv.5, the EPL activation was constant at 0.20, and grasp opening is plotted as a function of ECRB activation when the FDS activation was at either 0 or 0.1. The Table shows the grasp opening when the wrist was at either 5° extension or 10° extension. Depending on the ECRB activation level needed to reach the desired wrist angle, FDS activation can either increase grasp opening (e.g. when wrist angle = 10° extension), or decrease grasp opening (e.g. when wrist angle = 5° extension). Thus, both parameters must be inputs to the thumb module in order to obtain the desired grasp opening.

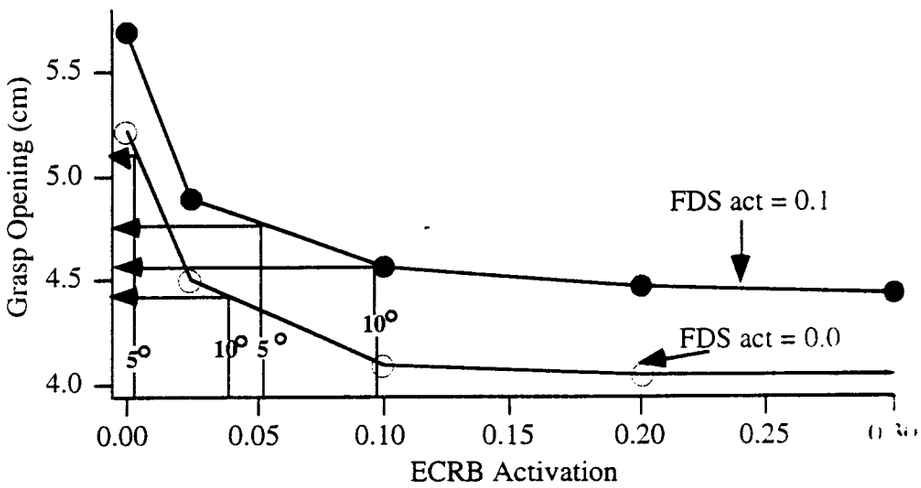

Figure 2.b.iv.5. Grasp opening as a function of ECRB activation for different activation levels of FDS when FPL activation was constant at 0.20. The arrows point to the grasp opening when the wrist was at either 5° extension or 10° extension.

FDS activation	wrist extension angle	required ECRB activation	grasp opening (cm)
0.1	10°	0.0979	4.57
0.0	10°	0.0441	4.20
0.1	5°	0.0589	4.65
0.0	5°	0.0037	5.10

Table 2.b.iv.1. Grasp opening and the required ECRB activation when the wrist was at 5° extension or 10° extension.

In terms of grasp force, wrist extension combined with radial deviation may increase grasp force (i.e. tenodesis). However since FDS activation will be constant by the time the thumb flexors are activated, the combination of FDS activation with wrist angle should not be a concern as it is with grasp opening.

As with the wrist module, training data for the thumb module was obtained with the dynamic model of the arm in two phases: one for grasp opening and one for grasp force. For grasp opening, the wrist was at either 0°, 5° extension, 10° extension, or 20° extension (wrist angle set by ECRB activation). The grasp opening was calculated when the EPL was activated at 0.065, 0.085, 0.1, 0.15, 0.2, and 0.3. These simulations were performed for FDS activation levels equal to 0.0, 0.05, and 0.1. The FPL, AdPo and AdPt were not activated in these simulations. For grasp force, the wrist was set at either 0° or 20° extension (by ECRB activation). The grasp force was calculated when the FPL, AdPo, and AdPt were activated in parallel at 0, 0.05, 0.1, 0.2, 0.25, and 0.3. The EPL was not activated in these simulations. FDS activation was constant at 0.1 since the fingers are flexed before the thumb flexors are activated in lateral grasp templates.

The training of the thumb module was performed in the same manner as with the wrist and finger module. The inputs to the radial basis network were wrist angle, FDS activation, grasp position (normalized), and grasp force (normalized). When grasp opening was being modulated during training (i.e. during EPL activation), the grasp force input to the module was set at 0 N. When grasp force was being modulated during training, (i.e. during FPL, AdPo, AdPt activation), grasp opening was set at 2.8

cm (distance between surface of thumb and index finger when the two are in contact with the external object). The outputs of the network were EPL activation, and FPL, AdPo, and AdPt activation (thumb flexors activated in parallel). When training the network, it was noticed that selecting an error criterion similar to the one for the wrist module resulted in a large number of hidden neurons. Consequently, the thumb module became too specific, and could not generalize to patterns not used in the training. Thus the error criteria was decreased to 0.04, which resulted in a smaller number of hidden neurons (19), but made the thumb module more generalized.

Performance of Interaction Networks in Isolating Hand Grasp and Wrist Control

Two examples of the performance of the trained feedforward controller are shown below. The first (Figure 2.b.iv.6) is a simulation of the grasp output with the wrist specified to be maintained at different angles during grasp, and the second tests the effects of gravity as an external disturbance.

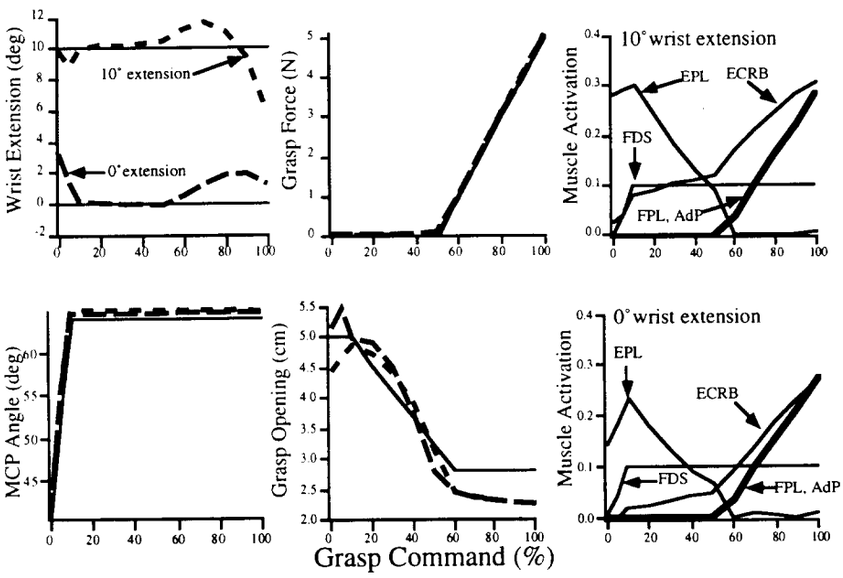

Figure 2.iv.b.6. Left four graphs: desired and simulated hand and wrist outputs *vs.* grasp command for two different values of wrist extension. Right two graphs: the muscle activation levels that produced the simulated outputs at the different command levels. Note that the grasp and wrist outputs matched the desired values closely, but that the interaction controller produced substantially different muscle activations for the EPL and ECRB for the two wrist angles.

In Figure 2.b.iv.6, the four left hand graphs show the desired and simulated wrist angle, index finger MCP angle, grasp force and grasp opening as functions of grasp command for two different cases. The first with a desired wrist angle of 10° extension, and the second with a desired wrist angle of 0° extension. The two graphs at the right show the muscle activations specified by the interaction networks for the two cases (10° at the top, 0° at the bottom). These are equivalent to pulse width maps. The grasp outputs and the wrist angles are all close to the desired values, indicating that the networks are compensating for the interactions. Note that the ECRB is modulated as a function of the grasp command to keep the wrist angle close to the desired value.

The extent of interaction and compensation can be observed in the activation maps. At the less extended wrist position, the acivation levels of the EPL and the ECRB are significantly decreased. Thus the interaction networks dynamically alter the activation maps to isolate the control of the hand and wrist. Since the recruitment properties of the simulated muscles are linear, the decreased activation can be interpreted directly as decreased muscle force (neglecting length tension and moment arm effects).

The second example (Figure 2.b.iv.7) shows the effect of gravity on the input-output properties. Since this is a feedforward control system, pronating the forearm increases wrist flexion because of the weight of the hand. (The forearm was in a neutral position for the training data, and for the simulations shown in the previous figure). On average, the wrist flexes about 4 to 5°, but the flexion does not significantly affect grasp output. Similarly, one would expect the wrist to extend if the forearm was supinated from neutral.

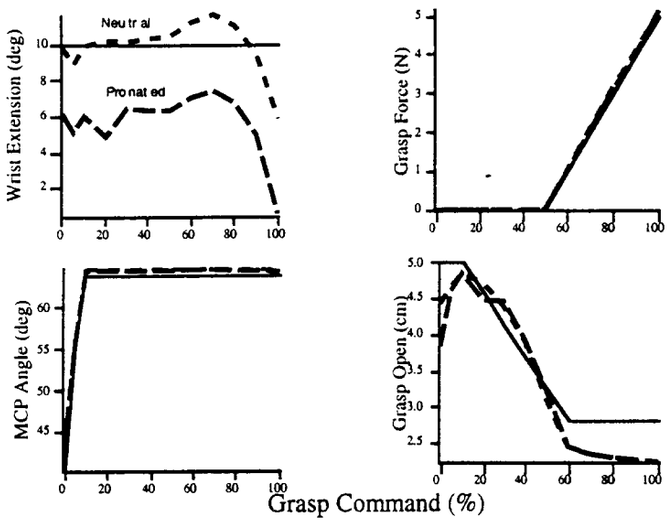

Figure 2.b.iv.7. The effect of gravity on wrist and hand grasp outputs. The interaction controller was the same as shown in the previous Figure; it was trained for the forearm in a neutral position, where gravity was in the ulnar direction. When the same inputs were applied with the forearm in the propnated position so that gravity produced a flexion meoment, the wrist assumed a more flexed position (about 4° across the range of grasp commands). There was almost no effect on the grasp output.

Plans for next quarter

We have demonstrated in simulation of lateral grasp that a feedforward controller can compensate for interactions between hand grasp and wrist posture that are learned from input-output data. This is data that can be measured experimentally. We need to test the system more extensively, particularly with a larger range of inputs and disturbances, and in palmar grasp.

References

Esteki, A., Mansour, J.M., "A dynamic model of the hand with application in functional neuromuscular stimulation", in press, Annals of Biomedical Engineering, 25(5), 1996.

Lemay, M.A. and Crago, P.E., "A dynamic model for simulating movements of the elbow, forearm, and wrist", J. Biomechanics, 29: 1319-1330, 1996.

Lemay, M.A. and Crago, P.E., "Feasibility of FNS wrist control in C4 and C5 tetraplegia", submitted to IEEE Trans. Rehab. Eng., 1996.

Kilgore, K.L. and Peckham, P.H., "Grasp synthesis for upper-extremity FNS .1. Automated method for synthesising the stimulus map", Medical & Biological Engineering & Computing, 31:607-614, 1993.